











Research Article

Synchronization of a New Chaotic System Using Adaptive Control: Design and Experimental Implementation

Alfredo Roldán-Caballero ¹, **J. Humberto Pérez-Cruz** ²,
Eduardo Hernández-Márquez ³, **José Rafael García-Sánchez** ⁴, **Mario Ponce-Silva** ⁵,
Jose de Jesus Rubio ², **Miguel Gabriel Villarreal-Cervantes** ⁶,
Jesús Martínez-Martínez ⁴, **Enrique García-Trinidad** ⁴,
and **Alejandro Mendoza-Chegue** ²

¹Unidad Profesional Interdisciplinaria de Ingeniería Campus Tlaxcala, Instituto Politécnico Nacional, Tlaxcala 90000, Mexico

²Sección de Estudios de Posgrado e Investigación, Escuela Superior de Ingeniería Mecánica y Eléctrica Unidad Azcapotzalco, Instituto Politécnico Nacional, Ciudad de México 02250, Mexico

³Departamento de Ingeniería Mecatrónica, Instituto Tecnológico Superior de Poza Rica, Tecnológico Nacional de México, Veracruz 93230, Mexico

⁴División de Ingeniería Mecatrónica, Tecnológico de Estudios Superiores de Huixquilucan, Tecnológico Nacional de México, La Magdalena Chichicapa, Estado de México 52773, Mexico

⁵Departamento de Ingeniería Electrónica, Tecnológico Nacional de México-CENIDET, Cuernavaca 62490, Morelos, Mexico

⁶Centro de Innovación y Desarrollo Tecnológico en Cómputo, Instituto Politécnico Nacional, Ciudad de México 07700, Mexico

Correspondence should be addressed to J. Humberto Pérez-Cruz; jhperez@ipn.mx

Received 25 December 2021; Revised 25 April 2022; Accepted 5 April 2023; Published 29 April 2023

Academic Editor: Viet-Thanh Pham

Copyright © 2023 Alfredo Roldán-Caballero et al. This is an open access article distributed under the Creative Commons Attribution License, which permits unrestricted use, distribution, and reproduction in any medium, provided the original work is properly cited.

This paper presents the design of an adaptive controller that solves the synchronization control problem of two identical Nwachioma chaotic systems in a master-slave configuration. The closed-loop stability is guaranteed by means of a Lyapunov-like analysis. With the aim of verifying the feasibility and performance of the proposed approach, a comparison with an active control algorithm is developed at the numerical simulation level. Based on such results, the master-slave Nwachioma chaotic system in closed-loop with adaptive control is now being experimentally tested by using two personal computers and two low-cost Arduino UNO boards. The experimental results not only show the good performance of the adaptive control but also that Arduino UNO boards are an excellent option for the experimental setup.

1. Introduction

It is well known that complex chaotic systems are nonlinear dynamic systems characterized by being nonperiodic oscillators with high sensitivity to initial conditions and whose solution can be hardly predictable in the long term [1, 2]. Despite the latter, these kind of systems are deterministic, meaning that suitable control algorithms can be designed for them [3, 4]. In this regard, the first chaotic system was

presented by Lorenz in [5]. From that moment on, several applications associated with chaotic systems have emerged. Some of those are in the areas of neurosystems [6, 7], chemical reactions [8, 9], secure communications [10–18], turbines [19, 20], robotics [21–24], cryptosystems [25–29], medicine [30–33], lasers [25, 34], among others.

When control strategies for complex chaotic systems are designed, the tasks to be solved can be divided into the following: (1) chaos suppression and (2) synchronization. The

present paper is focused on the second control task. Hence, the following state-of-the-art review describes some relevant contributions related to the synchronization of chaotic systems.

1.1. Related Works. The purpose of synchronization in chaotic systems is to achieve that one or more systems, with similar or different dynamics, converge to the same prescribed trajectory. Such a synchronization is generally carried out by means of a master-slave configuration. In this direction, the pioneer paper of Pecora and Carroll [35] described, for the first time, the synchronization of the Lorenz and the Rossler chaotic systems. Based on Pecora and Carroll's contribution, the research related to the design of controllers for synchronization of chaotic systems has been intensively studied during the last four decades [36–89]. The proposed control strategies reported in those works can be classified as active control [36–42], nonlinear control [43–57], linear feedback control [58–65], sliding modes [66–72], and adaptive control [73–89]. Such a literature is described below.

1.1.1. Active Control. Based on the literature, the active control approach was one of the first control methods for solving the synchronization problem. In this sense, Bai and Lonngren in [36, 37] demonstrated that coupled Lorenz systems can be synchronized by active control theory. The synchronization was verified at the simulation level. Meanwhile, Tang et al. [38] introduced a control strength matrix in the active control. With this extended method, the authors showed that the chaos complete synchronization can be achieved more easily. Numerical simulations on Rossler, Liu's four-scroll, and Chen systems confirmed the latter. Also, Yassen [39] presented simulation results of synchronizations between two different chaotic systems: the Lorenz and Lü systems, the Chen and Lü systems, and the Lorenz and Chen systems. On the other hand, Pérez-Cruz et al. [40] investigated the synchronization of a new three-dimensional chaotic system and, by means of Lyapunov analysis, a nonlinear controller was designed in such a way that the exponential convergence of the synchronization error was guaranteed and the results of the numeric simulation verified the good performance of this controller. In [41] Varan and Akful synchronized a hyperchaotic system and by using a Lyapunov function, achieved global asymptotic stability; numerical analysis was used to check the effectiveness of the proposed active control design. Lastly, Zhu and Du in [42] solved the antisynchronization of systems by using the active control, and the feasibility of control was verified via numerical simulations.

1.1.2. Nonlinear Control. Related to the design of nonlinear controllers for solving the synchronization problem, Suna et al. [43] proposed a nonlinear control strategy for synchronizing five chaotic systems, where the performance of the proposed approach was verified by numerical simulations. Zheng designed a nonlinear control in [44] to study multi-switching combination synchronization of three different chaotic systems, i.e., two drive chaotic systems and a controlled response chaotic system; simulation results depicted good performance

of the system in closed-loop. Likewise, Hettiarachchi et al. presented a nonlinear control algorithm for solving the synchronization problem over two time-delay coupled Hindmarsh–Rose neurons [45], whose effectiveness of the proposed approach was investigated through numerical simulations. Additionally, Yadav et al. [46] developed a nonlinear control method for combination-combination phase synchronization in fractional-order nonidentical complex chaotic systems. Simulation results were obtained, by using the Adams–Bashforth–Moulton method, with the aim of showing the performance of the system in closed-loop. Also, Yadav et al. [47] analyzed a nonlinear control for the triple compound synchronization among eight chaotic systems with external disturbances, and the feasibility of the proposed control was depicted through numerical simulations by using the Runge–Kutta method. Ouannas et al. [48] used a nonlinear control algorithm for the synchronization of a fractional hyperchaotic Rabinovich master-slave pair and numerical simulations demonstrated the validity and convergence of the proposed synchronization scheme. Whereas, Abdurahman and Jiang [49] introduced a nonlinear control strategy to investigate the general decay projective synchronization (GDPS) problem of a type of delayed memristor-based BAM neural networks; numerical results were obtained and the effectiveness of the proposed control was verified. On the other hand, Al-Hayali and Al-Azzawi [50] addressed the problem of synchronizing 4D identical Rabinovich hyperchaotic systems by using two strategies: active and nonlinear control; the good performance of the hyperchaotic systems in closed-loop was verified via simulation results. Another research was conducted by Al-Obeidi and Al-Azzawi [51], where they reported a nonlinear control strategy for chaos synchronization by using a 6D hyperchaotic system and numerical simulations were carried out to validate the effectiveness of the proposed control technique. Subsequently, Al-Azzawi and Al-Obeidi [52] provided a nonlinear control for a new 6D hyperchaotic system with real variables and a self-excited attractor. The proposed control allowed finding the stability of error dynamics and its performance was tested through numerical simulations. Also, Trikha et al. [53] introduced a novel 3D fractional chaotic system with two quadratic terms and designed a nonlinear control strategy for solving the synchronization problem; the simulations results demonstrated the effectiveness of the proposed strategy. Lin et al. [54] addressed the issue of global exponential synchronization for delayed impulsive and time-varying delayed inertial memristor-based quaternion-valued neural networks and the closed-loop system was verified via numerical simulations. Additionally, Jahanzaib et al. [55] elaborated a nonlinear control scheme for a novel fractional-order chaotic model with the aim of achieving the synchronization of the system; simulations were obtained and the good performance of the closed-loop system was demonstrated. Another work was developed by Ouannas et al. [48], where linear and nonlinear feedback controls were investigated and both force the slave system to follow the trajectory set by the master given different initial states; numerical simulations validated the synchronization schemes. Also, Ouannas et al. [56] developed two nonlinear control schemes to achieve asymptotic convergence with the aim of solving the

synchronization problem; experimental and simulation results supported the proposed theory. Later, Mesdoui et al. [57] designed nonlinear controls for solving the synchronization problem in a nonlinear bacterial cultures reaction-diffusion model and the effectiveness of the proposed control was verified via simulation results.

1.1.3. Linear Feedback Control. Regarding this kind of control, Wu [58] investigated the synchronization of the general master-slave identical generalized Lorenz systems, and the developed theory was validated via numerical simulations. Also, Yan and Yun [59] studied the synchronization of an LC chaotic system via three types of state feedback controls: (i) linear feedback control; (ii) adaptive feedback control; and (iii) a combination of linear feedback and adaptive feedback controls, where numerical simulations demonstrated the obtained theoretical results. Whereas, Rafikov and Balthazar in [60] formulated linear feedback controllers for the control and synchronization of chaos through an application of optimal control and Lyapunov stability theories to guarantee the global stability of the nonlinear error system; numerical simulations were provided in order to demonstrate the effectiveness of this control approach by achieving the synchronization of the hyperchaotic Rössler system. Later, Chen et al. [61] proposed the global synchronization criteria for a class of third-order nonautonomous chaotic systems consisting of cubic and (or) intersecting nonlinearity terms under the master-slave linear state error feedback control, whose effectiveness was verified through a numerical example. Likewise, Mobayen and Tchier [62] studied the chaos synchronization problem for a class of uncertain chaotic systems with Lipschitz nonlinearity conditions using an LMI-based state feedback stabilization control method and simulation results were given to show the efficiency of the control scheme. On the other hand, Zhao et al. addresses H_∞ synchronization for uncertain chaotic systems with one-sided Lipschitz nonlinearity under the output and intrinsic state delays [63], where numerical simulations proved the effectiveness of the proposed methodology by achieving the synchronization of Chua's circuit chaotic systems. Moreover, Mahmoud et al. [64] designed a single-state feedback track synchronization control algorithm and the effectiveness of the proposed algorithm is well illustrated via an exhaustive numerical simulation. Lastly, Azar et al. [65] explored the stabilization and synchronization of a chaotic system by means of a state feedback control that moves the eigenvalues of the linearized chaotic system to a point where the state variables reach equilibrium; numerical experiments and simulation results were reported with the aim of showing the effectiveness of the proposed approach.

1.1.4. Sliding Mode Control. Another control technique used for synchronization of chaotic systems is the sliding mode. For example, Siddique and Rehman [66] presented an adaptive integral sliding mode control design method for parameter identification and hybrid synchronization of chaotic systems connected in ring topology, where the effectiveness of the proposed technique was validated through

numerical examples. Also, Mufti et al. [67] developed the control design method for the transmission projective synchronization of multiple nonidentical coupled chaotic systems, whose performance in closed-loop was checked via numerical simulations. Another work was realized by Mufti et al. [68], where the synchronization and antisynchronization between the Chua and modified Chua oscillators were obtained and the effectiveness of the control strategies was validated via numerical simulations. Based on the Lyapunov stability theory and fractional-order integral sliding surface, a novel active sliding mode controller to synchronize fractional-order complex chaotic systems was proposed by Nian et al. [69] and was verified through numerical simulations. Another work was developed by Song et al. [70], where they focused on the robust synchronization issue for drive-response fractional-order chaotic systems applying the sliding mode control scheme; practical examples to illustrate the feasibility of the theoretical results are developed. In [71], Wan et al. proposed a discrete sliding mode controller to ensure the synchronization of chaotic systems and experimental results were given to demonstrate the performance of the proposed cryptosystems. The synchronization problem of chaotic systems using the integral-type sliding mode control for hyper-chaotic systems is considered in [72], where simulation results confirm the success of the designed control.

1.1.5. Adaptive Control. This approach is used when the parameters of the chaotic system are unknown. For example, Wu et al. [73] showed how adaptive controllers can be used to adjust the parameters of two Chua's oscillators to synchronize them via simulations. Whereas, based on the Lyapunov stability theory, Liao developed an adaptive control law [74] for synchronizing two Lorenz systems; the simulation results validated the proposed approach. In [75], Behinfaraz et al. developed a new fractional-order chaotic system where the parameter's adaption laws were obtained to design adaptive controllers using the Lyapunov stability theory and numerical examples were carried out to verify the performance of the controllers. By means of the Lyapunov theory, Wang et al. [76] proposed a nonlinear adaptive system to ensure the synchronization of two Hindmarsh-Rose neuron models and its simulation results verified the feasibility and effectiveness of the designed controller. Also, Pérez-Cruz [77] added a robustifying term to the adaptive control law for the stabilization and synchronization of an uncertain Zhang system; the performance of this robust approach was verified through numerical simulations. In [78], Khennaoui et al. proposed a one-dimensional adaptive control strategy that forces the states of discrete-time chaotic systems to tend asymptotically to zero; numerical results were presented to confirm the success of these synchronization schemes. Later, Luo et al. [79] proposed an adaptive synchronization scheme, which combines the best of the Chebyshev neural network, extended state tracking differentiator, and adaptive backstepping for the fractional-order chaotic arch microelectro-mechanical system; the effectiveness of the proposed adaptive synchronization scheme was demonstrated through simulation results. On the other hand, Xu et al. in [80] investigated an adaptive event-triggered

transmission strategy for the exponential synchronization of chaotic Lur'e systems; the designed control scheme was verified through numerical examples. Based on the complex-variable inequality and stability theory for the fractional-order complex-valued system, Zhang et al. presented [81] a new scheme for adaptive synchronization of fractional-order complex-variable chaotic systems with unknown complex parameters, where simulation results proved the effectiveness of the synchronization scheme. Liu et al. [82] developed the fractional Mittag-Leffler stability theory, that is, an adaptive, large-scale, and asymptotic synchronization control method for the synchronization of two different fractional-order chaotic systems under the conditions of determined parameters and uncertain parameters; the simulation results proved the good reliability of the controller. Another work was reported by Singh and Roy in [83] developed three different well-known control techniques: nonlinear active control, sliding mode control, and adaptive control, which are used for synchronization between various pairs of chaotic systems; simulation results are presented, which reflect the successful achievement of the objectives. In [84], Gao et al. proposed the cluster synchronization of a class of nonlinearly coupled Lur'e networks through a novel adaptive pinning control strategy, whose performance was depicted through numerical simulations. Another work was reported by Azar and Serrano in [85], where the design of an adaptive terminal sliding mode control for the stabilization of chaotic systems was proposed and experimental results were introduced for validating the control scheme. Javan et al. [86] showed a synchronization scheme using a robust-adaptive control procedure with the help of the Lyapunov stability theorem and the experimental results revealed the capability and flexibility of this method in synchronization of chaotic systems. Later, Javan et al. [87] developed an adaptive control method, and the definition of appropriate Lyapunov function was used for synchronization for chaotic systems; the results showed the effectiveness of the proposed synchronization technique in the medical images encryption for telemedicine application. One more piece of research was introduced by Wang and Rongwei [88], where they applied the adaptive control method to investigate the design of a universal controller to achieve the hybrid synchronization of a class of chaotic systems; numerical examples verify and validate the effectiveness of the proposed theoretical results. In addition, Khennaoui et al. [89] proposed adaptive control laws for solving the synchronization problem in three different types of chaotic systems, the Stefanski, Rossler, and Wang systems where the performance of the systems in closed-loop was verified by simulation results.

1.2. Discussion of Related Work, Motivation, and Contribution. The literature shows that several types of complex chaotic systems have been proposed with the aim of solving the synchronization control problem. The control strategies, usually developed, are active control [36–42], nonlinear control [43–57], linear feedback control [58–65], sliding modes [66–72], and adaptive control [73–89]. Also, on the one hand, it was observed that experimental results about synchronization of chaotic systems are

very scarce [90–97]. On the other hand, recently a new 3D chaotic system with four nonlinearities was proposed in [98]. Surprisingly, a control algorithm for solving the synchronization control problem for this system has not been yet proposed.

Motivated by the aforementioned and by the fact that complex chaotic systems can be applied in a wide range of fields, the contribution of this paper is to solve the synchronization for the chaotic system [98] by means of proposing an adaptive control. Moreover, with the purpose of enhancing this contribution, a comparison between an active control scheme and the adaptive control algorithm developed in this research is presented. Later, the experimental implementation of the adaptive control on the Nwachioma chaotic system is carried out through a novel experimental realization. For this latter, a low-cost testbed composed of two personal computers and two Arduino UNO boards along with MATLAB-Simulink are used.

The rest of the paper is structured as follows: in Section 2, the mathematical model of the new Nwachioma chaotic system in the master-slave configuration is presented and the adaptive control for solving the synchronization control problem is developed. The comparison between an active control and the adaptive control proposed here along with its experimental implementation is presented in Section 3. Finally, conclusions related to this research and future work are described in Section 4.

2. Materials and Methods

This section presents the generalities of the Nwachioma chaotic system and the master-slave configuration to be used throughout this paper. Also, the design of the adaptive control that achieves the synchronization of the master-slave configuration is introduced.

2.1. Nwachioma Chaotic System and Master-Slave Configuration. The Nwachioma chaotic system was proposed in [98]. The mathematical model describing its behavior is given by the following equations:

$$\begin{aligned}\dot{x}_1 &= a_1x_1 + a_2x_1x_3 + a_3x_2x_3, \\ \dot{x}_2 &= a_4x_2 + a_5x_1x_3 + a_6, \\ \dot{x}_3 &= a_7x_3 + a_8x_1^2x_2 + a_9,\end{aligned}\tag{1}$$

where a_i (for $i = 1, 2, \dots, 9$) are constants and $a_8x_1^2x_2$ assures the boundedness of the system [98]. As can be observed in the previous equations, the Nwachioma system is autonomous, i.e., the system does not have inputs that modify its dynamics. On the other hand, the behavior of such a system is purely chaotic when the following constant values are considered in (1):

$$\begin{aligned}a_1 &= -0.1, a_2 = 0.15, a_3 = 0.18, a_4 = 3.9, \\ a_5 &= -1.5, a_6 = -4, a_7 = -4.9, a_8 = 2.5, a_9 = 0,\end{aligned}\tag{2}$$

and also when the initial conditions are set to $x_1(0) = 1$, $x_2(0) = 3$, and $x_3(0) = 8$ (see Figure 1).

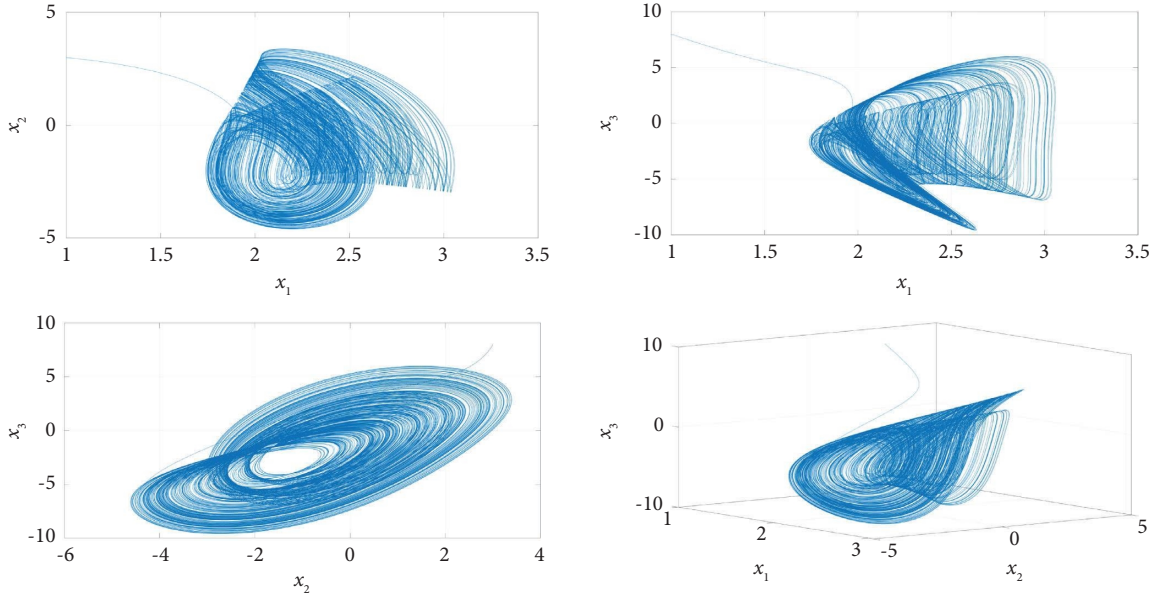


FIGURE 1: Planes and phase portraits of the Nwachioma chaotic system, where the self-attractor of the system can be observed. The initial conditions considered for the plane and the phase portrait are $x_1(0) = 1$, $x_2(0) = 3$, and $x_3(0) = 8$.

As can be observed in Figure 1, the planes and phase portraits of system (1) show the self-excited attractor, meaning that the states of the system are bounded over a specific region. It is worth mentioning that the system is very sensitive to initial conditions due to the chaoticity of its dynamics. This can be confirmed through the simulation results depicted in Figure 2. Such results show the behavior of the Nwachioma system when two sets of initial conditions are used. The first set of initial conditions were reported in [98] and were defined as $x_1(0) = 1$, $x_2(0) = 3$, and $x_3(0) = 8$, whereas the second set are those proposed in this paper and are prescribed to be $x_{1b}(0) = 1$, $x_{2b}(0) = 3.002$, and $x_{3b}(0) = 8$.

The master-slave Nwachioma chaotic system is composed of two subsystems: a master Nwachioma system and a slave Nwachioma-alike system. The first one is defined by the following autonomous dynamics:

$$\begin{aligned}\dot{x}_{1m} &= a_1 x_{1m} + a_2 x_{1m} x_{3m} + a_3 x_{2m} x_{3m}, \\ \dot{x}_{2m} &= a_4 x_{2m} + a_5 x_{1m} x_{3m} + a_6, \\ \dot{x}_{3m} &= a_7 x_{3m} + a_8 x_{1m}^2 x_{2m} + a_9,\end{aligned}\quad (3)$$

and it is identified through the subscript m . On the other hand, the slave system is denoted with the subscript s and, compared with the master, it is not an autonomous system, since it is commanded through inputs u_1 , u_2 , and u_3 . The dynamics of the slave is defined as follows:

$$\begin{aligned}\dot{x}_{1s} &= a_1 x_{1s} + a_2 x_{1s} x_{3s} + a_3 x_{2s} x_{3s} + u_1, \\ \dot{x}_{2s} &= a_4 x_{2s} + a_5 x_{1s} x_{3s} + a_6 + u_2, \\ \dot{x}_{3s} &= a_7 x_{3s} + a_8 x_{1s}^2 x_{2s} + a_9 + u_3,\end{aligned}\quad (4)$$

where constants a_i are equal in both systems. However, when the adaptive control is designed such constants are considered to be unknown.

2.2. Adaptive Synchronization. The objective of the adaptive synchronization control proposed in this section is to achieve that $(x_{1s}, x_{2s}, x_{3s}) \rightarrow (x_{1m}, x_{2m}, x_{3m})$. For such an aim, the following synchronization errors are defined:

$$\begin{aligned}e_1 &= x_{s1} - x_{m1}, \\ e_2 &= x_{s2} - x_{m2}, \\ e_3 &= x_{s3} - x_{m3}.\end{aligned}\quad (5)$$

Thus, from (5), the error dynamics is given by

$$\begin{aligned}\dot{e}_1 &= \dot{x}_{s1} - \dot{x}_{m1}, \\ \dot{e}_2 &= \dot{x}_{s2} - \dot{x}_{m2}, \\ \dot{e}_3 &= \dot{x}_{s3} - \dot{x}_{m3}.\end{aligned}\quad (6)$$

After replacing the dynamics (3) and (4) in (6), the following error dynamics in open-loop is obtained:

$$\begin{aligned}\dot{e}_1 &= a_1 x_{s1} + a_2 x_{s1} x_{s3} + a_3 x_{s2} x_{s3} + u_1 - (a_1 x_{m1} + a_2 x_{m1} x_{m3} + a_3 x_{m2} x_{m3}), \\ \dot{e}_2 &= a_4 x_{m2} + a_5 x_{s1} x_{s3} + a_6 + u_2 - (a_4 x_{m2} + a_5 x_{m1} x_{m3} + a_6), \\ \dot{e}_3 &= a_7 x_{s3} + a_8 x_{s1}^2 x_{s2} + a_9 + u_3 - (a_7 x_{m3} + a_8 x_{m1}^2 x_{m2} + a_9).\end{aligned}\quad (7)$$

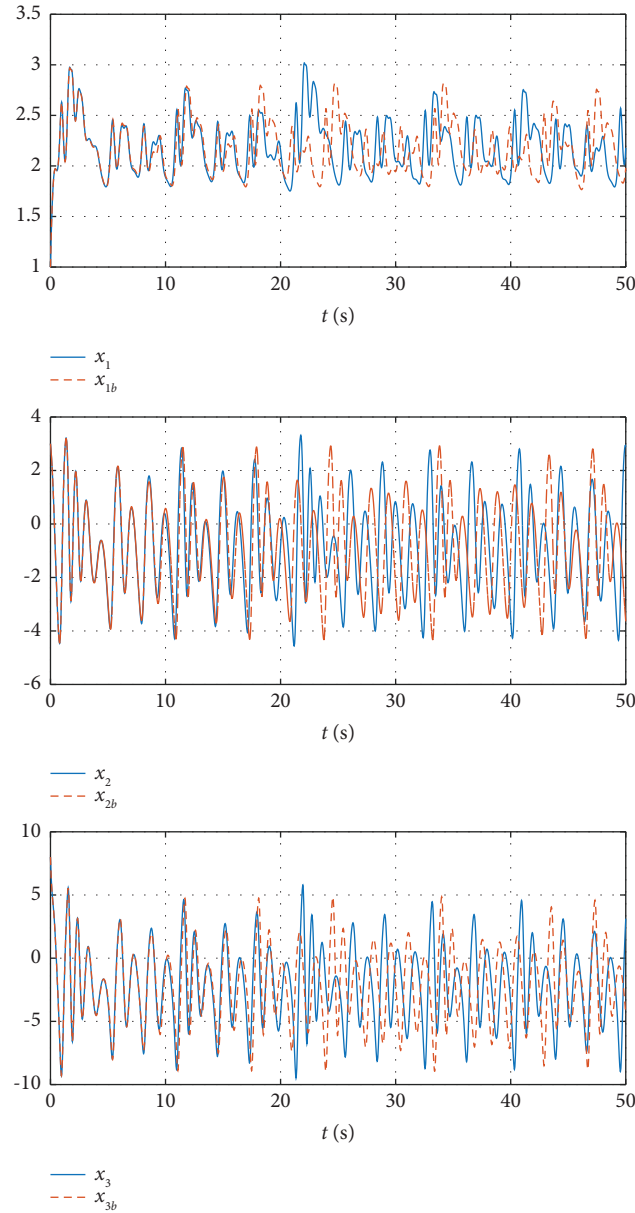


FIGURE 2: Simulation results showing the sensitivity of the Nwachioma chaotic system when small variations are considered in the initial conditions. The initial conditions considered in this simulation are $x_1(0) = 1$, $x_2(0) = 3$, $x_3(0) = 8$, $x_{1b}(0) = 1$, $x_{2b}(0) = 3.002$, and $x_{3b}(0) = 8$.

Lastly, by considering (5) into (7), the error dynamics in open-loop can be expressed in terms of the master dynamics and the synchronization errors as follows:

$$\begin{aligned}
 \dot{e}_1 &= a_1 e_1 + a_2 (e_1 e_3 + x_{m3} e_1 + x_{m1} e_3) + a_3 (e_2 e_3 + x_{m2} e_3 + x_{m3} e_2) + u_1, \\
 \dot{e}_2 &= a_4 e_2 + a_5 (e_1 e_3 + x_{m1} e_3 + x_{m3} e_1) + u_2, \\
 \dot{e}_3 &= a_7 e_3 + a_8 (e_1^2 e_2 + 2x_{m1} e_1 + x_{m1}^2 e_2 + x_{m2} e_1^2 + 2x_{m1} x_{m2} e_1) + u_3.
 \end{aligned} \tag{8}$$

2.2.1. *Adaptive Control Design.* With the intention of achieving that the slave subsystem tracks the master

subsystem, i.e., $(x_{1s}, x_{2s}, x_{3s}) \longrightarrow (x_{1m}, x_{2m}, x_{3m})$, the following adaptive inputs u_1 , u_2 , and u_3 are designed:

$$\begin{aligned} u_1 &= -\hat{a}_1 e_1 - \hat{a}_2 (e_1 e_3 + x_{m3} e_1 + x_{m1} e_3) - \hat{a}_3 (e_2 e_3 + x_{m2} e_3 + x_{m3} e_2) - k_1 e_1, \\ u_2 &= -\hat{a}_4 e_2 - \hat{a}_5 (e_1 e_3 + x_{m1} e_3 + x_{m3} e_1) - k_2 e_2, \\ u_3 &= -\hat{a}_7 e_3 - \hat{a}_8 (e_1^2 e_2 + 2x_{m1} e_1 + x_{m1}^2 e_2 + x_{m2} e_1^2 + 2x_{m1} x_{m2} e_1) - k_3 e_3. \end{aligned} \quad (9)$$

where \hat{a}_i (for $i = 1, 2, 3, 4, 5, 7, 8$) are the estimated parameters and gains k_i (for $i = 1, 2, 3$) are greater than zero. When replacing (9) in (8), and after defining the error in the

unknown parameters as $\tilde{a}_i = \hat{a}_i - a_i$ (for $i = 1, 2, 3, 4, 5, 7, 8$), then the following error dynamics in closed-loop is obtained:

$$\begin{aligned} \dot{e}_1 &= -\tilde{a}_1 e_1 - \tilde{a}_2 (e_1 e_3 + x_{m3} e_1 + x_{m1} e_3) - \tilde{a}_3 (e_2 e_3 + x_{m2} e_3 + x_{m3} e_2) - k_1 e_1, \\ \dot{e}_2 &= -\tilde{a}_4 e_2 - \tilde{a}_5 (e_1 e_3 + x_{m1} e_3 + x_{m3} e_1) - k_2 e_2, \\ \dot{e}_3 &= -\tilde{a}_7 e_3 - \tilde{a}_8 (e_1^2 e_2 + 2x_{m1} e_1 + x_{m1}^2 e_2 + x_{m2} e_1^2 + 2x_{m1} x_{m2} e_1) - k_3 e_3. \end{aligned} \quad (10)$$

2.2.2. *Stability Proof and Learning law.* For demonstrating the stability of the closed-loop system (10) by means of the Lyapunov theory, the first step is to propose and analyze an energy candidate function defined in terms of states e_i (for $i = 1, 2, 3$) and parameters \tilde{a}_i . Thus, the following function is proposed:

$$V(t) = \frac{1}{2} \left(\sum_{i=1}^3 e_i^2 + \sum_{i=1}^5 \tilde{a}_i^2 + \sum_{i=7}^8 \tilde{a}_i^2 \right). \quad (11)$$

With the aim of verifying the stability of the closed-loop system (10), the time-derivative of (11) along with (10) must be analyzed [99]; that is,

$$\begin{aligned} \dot{V}(t) &= \tilde{a}_1 [\dot{\hat{a}}_1 - e_1^2] + \tilde{a}_2 [\dot{\hat{a}}_2 - (e_1^2 e_3 + x_{m3} e_1^2 + x_{m1} e_1 e_3)] \\ &\quad + \tilde{a}_3 [\dot{\hat{a}}_3 - (e_1 e_2 e_3 + x_{m2} e_1 e_3 + x_{m3} e_1 e_2)] - k_1 e_1^2 + \tilde{a}_4 [\dot{\hat{a}}_4 - e_2^2] \\ &\quad + \tilde{a}_5 [\dot{\hat{a}}_5 - (e_1 e_2 e_3 + x_{m1} e_2 e_3 + x_{m3} e_1 e_2)] - k_2 e_2^2 + \tilde{a}_7 [\dot{\hat{a}}_7 - e_3^2] \\ &\quad + \tilde{a}_8 [\dot{\hat{a}}_8 - (e_1^2 e_2 e_3 + 2x_{m1} e_1 e_3 + x_{m1}^2 e_2 e_3 + x_{m2} e_1^2 e_3 + 2x_{m1} x_{m2} e_1 e_3)] - k_3 e_3^2. \end{aligned} \quad (12)$$

Now, it is easily observed that a suitable learning law for parameter estimation is the following:

$$\begin{aligned} \dot{\hat{a}}_1 &= e_1^2, \\ \dot{\hat{a}}_2 &= e_1^2 e_3 + x_{m3} e_1^2 + x_{m1} e_1 e_3, \\ \dot{\hat{a}}_3 &= e_1 e_2 e_3 + x_{m2} e_1 e_3 + x_{m3} e_1 e_2, \\ \dot{\hat{a}}_4 &= e_2^2, \\ \dot{\hat{a}}_5 &= e_1 e_2 e_3 + x_{m1} e_2 e_3 + x_{m3} e_1 e_2, \\ \dot{\hat{a}}_7 &= e_3^2, \\ \dot{\hat{a}}_8 &= e_1^2 e_2 e_3 + 2x_{m1} e_1 e_3 + x_{m1}^2 e_2 e_3 + x_{m2} e_1^2 e_3 + 2x_{m1} x_{m2} e_1 e_3. \end{aligned} \quad (13)$$

After replacing (13) in (12), the following is obtained:

$$\dot{V}(t) = -k_1 e_1^2 - k_2 e_2^2 - k_3 e_3^2. \quad (14)$$

Notice that (14) is negative semidefinite, i.e., $\dot{V}(t) \leq 0$. Hence, system (10) is stable in the sense of Lyapunov [99].

However, with the aim of demonstrating the asymptotic stability of (10) the Barbalat's lemma needs to be invoked [100].

Lemma 1 (Barbalat's Lemma). *If $e(t): \mathbb{R}^+ \longrightarrow \mathbb{R}^+$ is uniformly continuous for $t \geq 0$ and if*

$$\lim_{t \rightarrow \infty} \int_0^t \|e(\tau)\| d\tau \leq \epsilon, \quad (15)$$

for $\epsilon \in \mathbb{R}^+$, then

$$\lim_{t \rightarrow \infty} e(t) = 0. \quad (16)$$

Corollary 1. *If $e(t) \in L_2 \cap L_\infty$ and $\dot{e}(t) \in L_\infty$, then*

$$\lim_{t \rightarrow \infty} e(t) = 0. \quad (17)$$

From Corollary 1 and when replacing $k = \min \{k_1, k_2, k_3\}$ in (14), the following is obtained:

$$\dot{V} \leq -k(e_1^2 + e_2^2 + e_3^2). \quad (18)$$

Now, after integrating from 0 to t both sides of (18),

$$\int_0^t (e_1^2 + e_2^2 + e_3^2) d\tau \leq \frac{V(0) - V(t)}{k}, \quad (19)$$

and since $V(t) > 0$, it means that $V(0) - V(t) < V(0)$. Hence,

$$\frac{V(0) - V(t)}{k} < \frac{V(0)}{k}. \quad (20)$$

When replacing the latter expression in (19) and after finding \lim when $t \rightarrow \infty$, then

$$\lim_{t \rightarrow \infty} \int_0^t (e_1^2 + e_2^2 + e_3^2) d\tau \leq \frac{V(0)}{k}. \quad (21)$$

Thus, it is concluded that

$$e_i \in L_2. \quad (22)$$

In the following, the rest of conditions related to Corollary 1 are verified. By considering that $\dot{V}(t) \leq 0$ and after integrating such an expression from 0 to t , it is found that $V(t) \leq V(0)$. Also, it is observed that $V(t)$ is bounded since $V(t) > 0$. Thus, from (11) e_i and \tilde{a}_i are also bounded and, consequently,

$$e_i \in L_\infty. \quad (23)$$

On the other hand, since e_i , \tilde{a}_i , and the master system (3) are bounded (it is worth remembering that the vector state of a chaotic system is bounded), then \dot{e}_i in (10) is also bounded. Thus,

$$\dot{e}_i \in L_\infty. \quad (24)$$

Lastly, after considering (22), (23), and (24), it is easily observed that Lemma 1 guarantees that

$$\lim_{t \rightarrow \infty} e_i(t) = 0. \quad (25)$$

Remark 1. Note that the estimation errors \tilde{a}_i are bounded but not tend to zero; however, the errors e_i does tend to zero when the time is large enough, as will be shown in the next section.

Remark 2. It is important to mention that according to the previous proof, from a strictly theoretical point of view, the synchronization can be achieved for any value of the system

constant parameters a_i whenever the control gains are $k_1 > 0$, $k_2 > 0$, and $k_3 > 0$.

3. Results

In order to enhance the contribution of this paper, in this section, a comparison between an active control scheme and the adaptive control algorithm previously developed in Section 2 is presented. Such a comparison is executed via simulation results with the aim of verifying the performance in closed-loop of the Nwachioma chaotic system, in master-slave configuration, with both controls. Later, the experimental implementation of the adaptive control on the Nwachioma chaotic system is carried out through a novel experimental realization.

3.1. Comparison with respect to Active Control. Although active control was one of the first methods proposed for solving the synchronization problem, currently, is still frequently used [101–105]. This method can be considered a kind of feedback linearization one. Active control comprises two stages: one for compensation of nonlinearities and another one for decoupling. In this regard, and with the purpose of executing the comparison with the adaptive control developed in this paper; in the following, an active control is designed for solving the synchronization problem associated with the Nwachioma chaotic system.

3.1.1. Design of the Active Control. With the intention of avoiding any kind of confusion regarding both control algorithms, i.e. the adaptive control and the active control, new variables are defined for the design of the active control. Now the slave system, where the active control is applied, has the following dynamics:

$$\begin{aligned} \dot{x}_{a1s} &= a_1 x_{a1s} + a_2 x_{a1s} x_{a3s} + a_3 x_{a2s} x_{a3s} + u_{a1}, \\ \dot{x}_{a2s} &= a_4 x_{a2s} + a_5 x_{a1s} x_{a3s} + a_6 + u_{a2}, \\ \dot{x}_{a3s} &= a_7 x_{a3s} + a_8 x_{a1s}^2 x_{a2s} + a_9 + u_{a3}, \end{aligned} \quad (26)$$

whereas the tracking error is given by

$$\begin{aligned} e_{a1} &= x_{a1s} - x_{m1}, \\ e_{a2} &= x_{a2s} - x_{m2}, \\ e_{a3} &= x_{a3s} - x_{m3}. \end{aligned} \quad (27)$$

By considering (26) and (27), the following error dynamics in open-loop is obtained:

$$\begin{aligned} \dot{e}_{a1} &= a_1 e_{a1} + a_2 (e_{a1} e_{a3} + x_{m3} e_{a1} + x_{m1} e_{a3}) + a_3 (e_{a2} e_{a3} + x_{m2} e_{a3} + x_{m3} e_{a2}) + u_{a1}, \\ \dot{e}_{a2} &= a_4 e_{a2} + a_5 (e_{a1} e_{a3} + x_{m1} e_{a3} + x_{m3} e_{a1}) + u_{a2}, \\ \dot{e}_{a3} &= a_7 e_{a3} + a_8 (e_{a1}^2 e_{a2} + 2x_{m1} e_{a1} + x_{m1}^2 e_{a2} + x_{m2} e_{a1}^2 + 2x_{m1} x_{m2} e_{a1}) + u_{a3}. \end{aligned} \quad (28)$$

In (28), note the nonlinearities and the coupling of the variables. Hence, the following active control is proposed:

$$\begin{aligned}
u_{a1} &= -a_1 e_{a1} - a_2 (e_{a1} e_{a3} + x_{m3} e_{a1} + x_{m1} e_{a3}) - a_3 (e_{a2} e_{a3} + x_{m2} e_3 + x_{m3} e_{a2}) - k_1 e_{a1}, \\
u_{a2} &= -a_4 e_{a2} - a_5 (e_{a1} e_{a3} + x_{m1} e_{a3} + x_{m3} e_{a1}) - k_2 e_{a2}, \\
u_{a3} &= -a_7 e_{a3} - a_8 (e_{a1}^2 e_{a2} + 2x_{m1} e_{a1} + x_{m1}^2 e_{a2} + x_{m2} e_{a1}^2 + 2x_{m1} x_{m2} e_{a1}) - k_3 e_{a3}.
\end{aligned} \tag{29}$$

After replacing the proposed control (29) in the error dynamics (28), the following error dynamics in closed-loop is obtained:

$$\begin{aligned}
\dot{e}_{a1} &= -k_1 e_{a1}, \\
\dot{e}_{a2} &= -k_2 e_{a2}, \\
\dot{e}_{a3} &= -k_3 e_{a3}.
\end{aligned} \tag{30}$$

It is easily observed that the dynamics (30) is linear and the time-varying error variables are decoupled. Additionally, if $k_1 > 0$, $k_2 > 0$, and $k_3 > 0$, then $(e_{a1}, e_{a2}, e_{a3}) \rightarrow (0, 0, 0)$.

3.1.2. Simulation Results. On the one hand, the efficiency of both controls, the adaptive one and the active one, is validated by using the criterion of the quadratic error integral as an index performance. For the adaptive control, the index performance is defined as

$$\phi(t) = \int_0^t (e_1^2 + e_2^2 + e_3^2) d\xi, \tag{31}$$

whereas the index performance for the active control is defined as

$$\phi_a(t) = \int_0^t (e_{a1}^2 + e_{a2}^2 + e_{a3}^2) d\xi. \tag{32}$$

By using these indexes it is possible to obtain a measure, for comparative purposes, between both controls. Such a measure allows to observe graphically the sum of both errors, the transient one and the stable one (if exists). On the other hand, with the intention of comparing the performance of the adaptive control and the active control, four simulations are carried out when the parameters a_i defined in (2) of the master-slave Nwachiona chaotic system are changed according to the values specified in Table 1.

The rest of parameters for the active control (29) were defined previously in (2) and were given as

$$\begin{aligned}
a_1 &= -0.1, a_2 = 0.15, a_3 = 0.18, a_4 = 3.9, \\
a_5 &= -1.5, a_6 = -4, a_7 = -4.9, a_8 = 2.5, a_9 = 0.
\end{aligned} \tag{33}$$

The gains of both controls were chosen as $(k_1, k_2, k_3) = (1, 1, 1)$, while the initial conditions for the master system were defined as $(x_{1m}(0), x_{2m}(0), x_{3m}(0)) = (1, 3, 8)$, the initial conditions for the slave system when using the adaptive control were selected as $(x_{1s}(0), x_{2s}(0), x_{3s}(0)) = (0, 0, 0)$, and those for the same slave system when using the active control were selected as $(x_{1as}(0), x_{2as}(0), x_{3as}(0)) = (0, 0, 0)$. All simulations were executed in MATLAB-Simulink with the variable-step solver ode23s.

(a) Numerical simulation 1: The results presented in Figure 3 show that both control algorithms solved

the synchronization control task. This is accomplished because the parameters of the Nwachiona chaotic system, in the master-slave configuration, and those of the active control were the same.

- (b) Numerical simulation 2: Figure 4 depicts the performance of the Nwachiona chaotic system in closed-loop with both controls, the adaptive one and the active one. Although the synchronization control task is achieved, the transient response of the slave system due to the active control is greater than the one obtained in the previous simulation.
- (c) Numerical simulation 3: As can be observed in Figure 5, the synchronization control task is solved for the master-slave Nwachiona chaotic system in closed-loop with the adaptive control. However, such a task is not solved for the active control.
- (d) Numerical simulation 4: Similar to the previous simulation results, those presented in Figure 6 show that the chaotic system in closed-loop with the adaptive control solved the synchronization control problem. But when using the active control the synchronization is not achieved. It is worth mentioning that this numerical simulation was executed only for 4 s, since $x_{a2s} \rightarrow \infty$ and $\phi_a(t) \rightarrow \infty$ when $t \rightarrow \infty$, as can be observed in Figure 6.

3.1.3. Comments on the Numerical Simulations. As can be noted in Figures 3–6, the adaptive control exhibits a better performance compared with the performance achieved by the active control. Such a superior behavior on the closed-loop Nwachiona system, in the master-slave configuration, with the adaptive control is observed through the performance indexes of the quadratic error integral calculated for both controls. The results associated with the indexes $\phi(t)$ and $\phi_a(t)$, for each numerical simulation, are shown in Table 2.

3.2. Experimental Implementation. With the aim of highlighting the effectiveness of the adaptive control (9) developed in this paper, a novel and easy to understand implementation in closed-loop of the proposed approach with the Nwachiona chaotic system, in the master-slave configuration, is presented in this section. The experimental realization of the adaptive control is carried out by using MATLAB-Simulink and two computers, one for the master system and a second one for the slave system. The testbed is depicted in Figure 7, where the connections diagram between the master computer and the slave computer along with their corresponding Arduino UNO boards are shown.

TABLE 1: Changes in parameters a_i for comparison purposes between the adaptive control and the active control via numerical simulations.

	a_1	a_2	a_3	a_4	a_5	a_6	a_7	a_8	a_9
Numerical simulation 1	-0.10	0.15	0.180	3.90	-1.5	-4	-4.90	2.5	0
Numerical simulation 2	-0.14	0.21	0.252	5.46	-2.1	-5.6	-6.86	3.5	0
Numerical simulation 3	-0.18	0.27	0.324	7.02	-2.7	-7.2	-8.82	4.5	0
Numerical simulation 4	-0.22	0.33	0.396	8.58	3.3	-8.8	-10.78	5.5	0

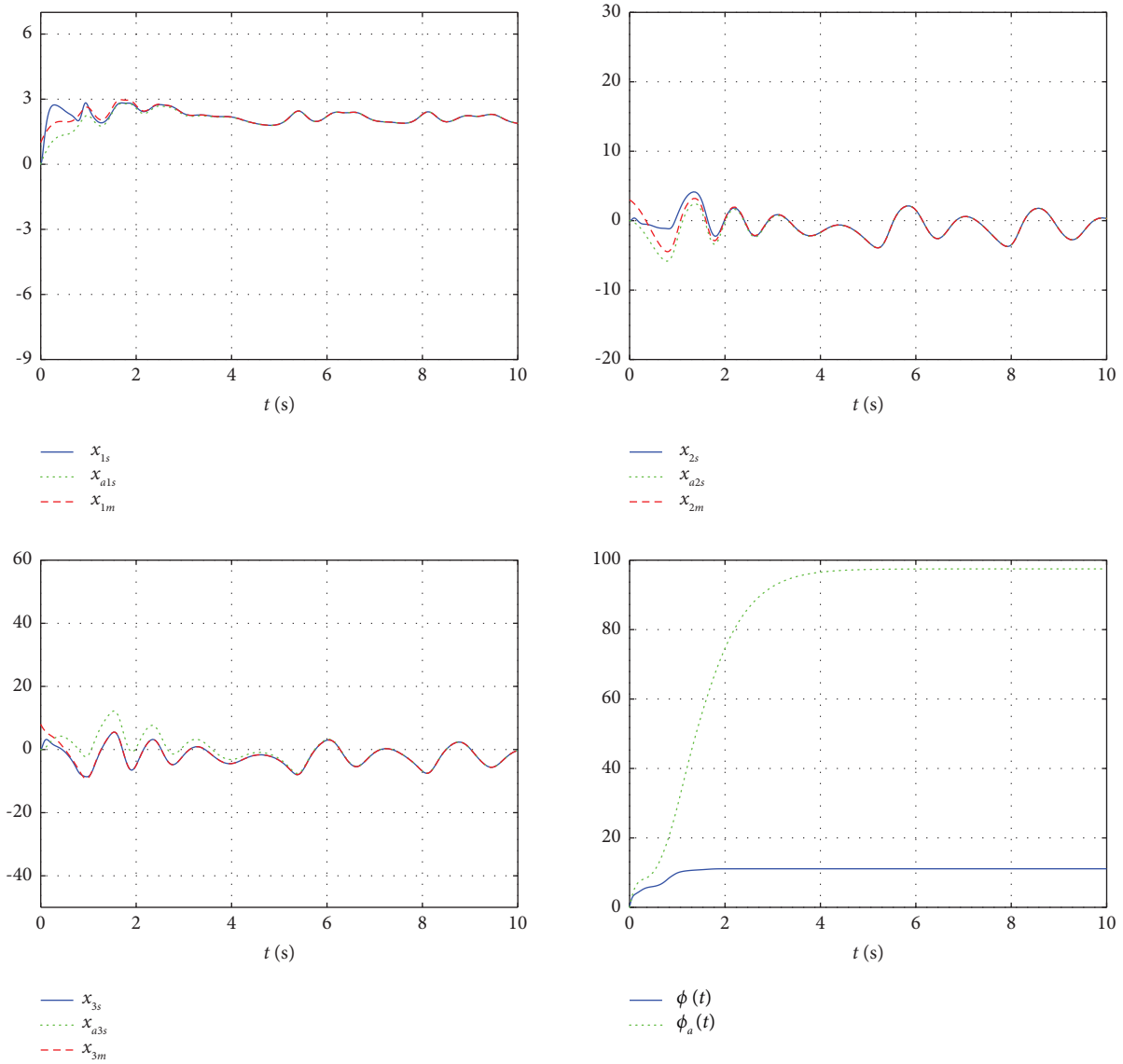


FIGURE 3: Numerical simulation 1. Comparison between the adaptive control and the active control in closed-loop with the Nwachioma chaotic system. The used parameters are in accordance with those specified on the first line in Table 1. The indexes obtained for this simulation are $\phi(10\text{ s}) = 11.11$ and $\phi_a(10\text{ s}) = 97.48$.

The master system and the slave system are implemented by programming their mathematical models (3) and (4), respectively, in MATLAB-Simulink by using the numeric method ode4 with sampling step of 1 ms. Both the computers are interconnected via the serial communication protocol RS-232 along with two Arduino UNO development boards [106]. It is worth mentioning that using MATLAB-Simulink along with the RS-232 serial protocol and the

Arduino UNO board is, indeed, a low-cost implementation of the approach presented in this paper. In fact, the synchronization problem in chaotic systems is tremendously affordable when using these kind of computational tools.

3.2.1. Synchronization of the Master-Slave Nwachioma Chaotic System. The synchronization of the master-slave Nwachioma chaotic system is realized through the

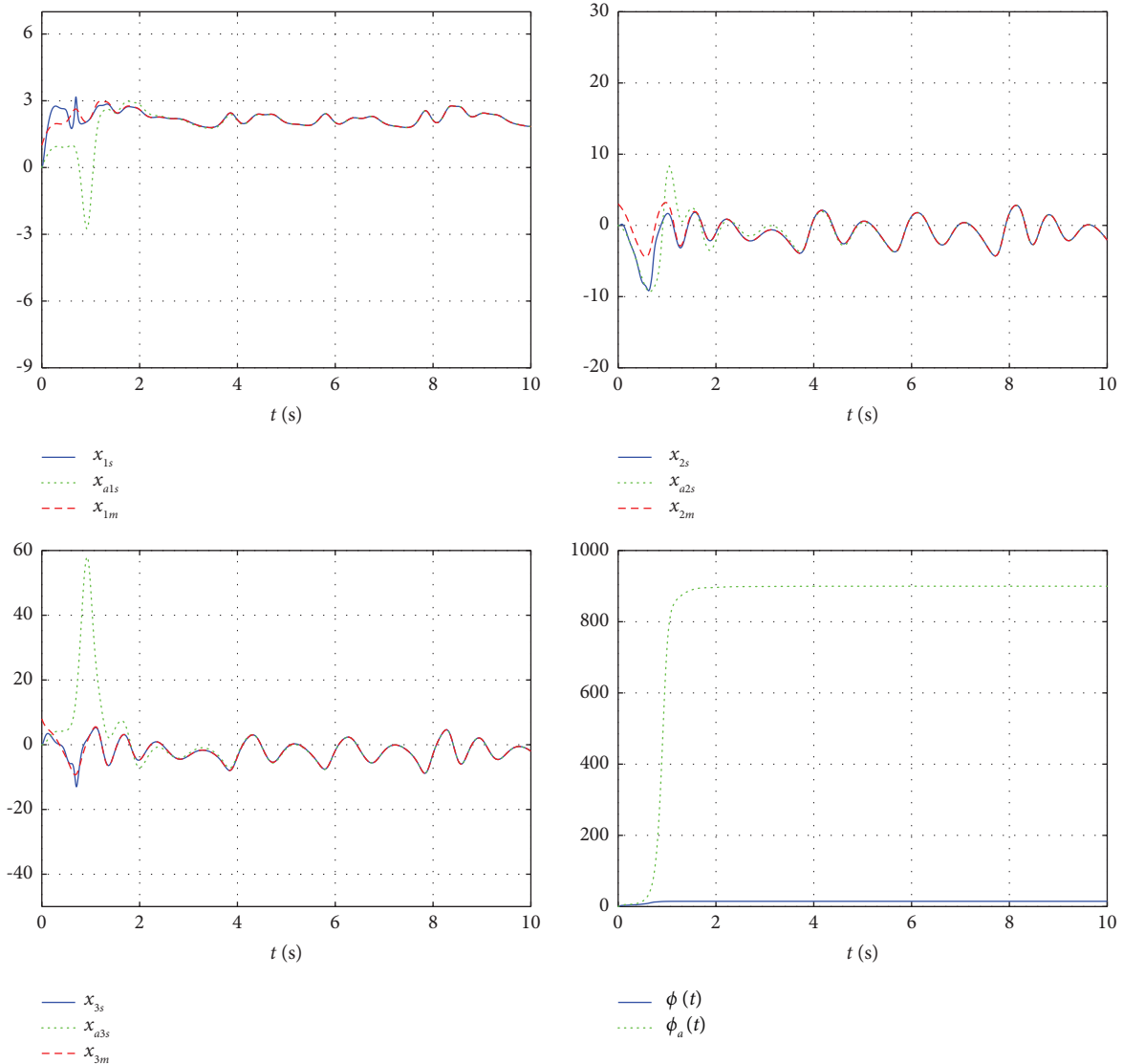


FIGURE 4: Numerical simulation 2. Results of the adaptive control and the active control in closed-loop with the Nwachioma chaotic system. The used parameters are in accordance with those specified on the second line in Table 1. The indexes obtained for this simulation are $\phi(10\text{ s}) = 14.76$ and $\phi_a(10\text{ s}) = 899.7$.

connections shown in Figure 7, whereas the flowchart shown in Figure 8 depicts the process to be followed for achieving the communication between the master system and the slave system.

It is worth noticing that for achieving the synchronization of the chaotic system, the Arduino UNO boards and the computers must be configured. In this regard, the Arduino UNO boards are interconnected to each other by using a virtual serial port. The code shown in the Listing 1 commands both Arduino UNO boards and establishes the flow of information, i.e., master computer-board-board-slave computer. The virtual port directs the communication between both Arduino boards. The data are received from the virtual (or the physical) serial port and are saved and sent via the variable *InData* to the remaining serial port, respectively.

On the one hand, Computer 1 is interconnected to the Arduino UNO 1 board via a USB cable, where the Arduino driver is used so that the connection is viewed as a serial port. On the other hand, both Arduino UNO boards are interconnected through pins RX and TX, as can be observed in the code presented in the Listing 1. This is the RX pin of the first board, which is connected to the TX pin and vice versa. Lastly, the Arduino UNO 2 board is connected to Computer 2 in the same way as computer 1 is connected to its corresponding Arduino board.

Once the connections have been made, the next step is the implementation of dynamics associated with the master system (3) and the slave system (4) in computer 1 and computer 2, respectively. Figure 9 depicts the block diagram programmed in MATLAB-Simulink with the intention of acquiring the response of master system (3) and send it to

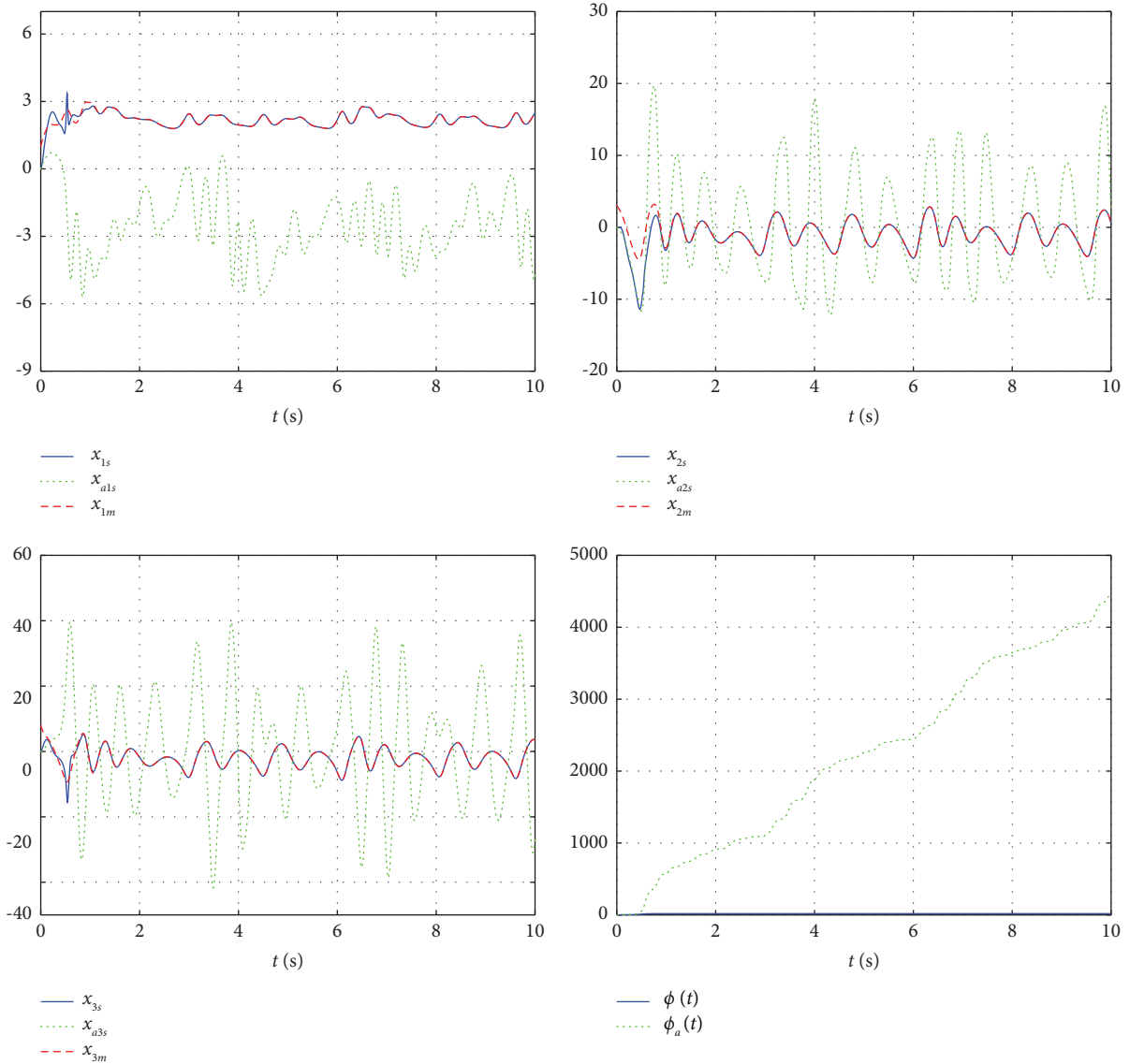


FIGURE 5: Numerical simulation 3. Comparison between the adaptive control and the active control in closed-loop with the Nwachioma chaotic system. The used parameters are in accordance with those specified on the third line in Table 1. The indexes obtained for this simulation are $\phi(10 \text{ s}) = 18.57$ and $\phi_a(10 \text{ s}) = 4490$.

computer 2. Since the two Nwachioma systems of the master-slave configuration are equal, the parameters (2) are programmed in both systems for implementation purposes. However, such parameters are considered to be unknown and, consequently, are not used by the adaptive control (9).

In the following, the block diagram of Figure 9 is described.

- (i) Nwachioma master system: This block is composed of the blocks a_i , *Master*, and *Integrator*. The block a_i contains this constant parameters of the system (3), considered to be unknown. However, for implementation purposes, the parameters a_i given by (2) are programmed instead. The equations (3) are programmed in *Master* block, whose output is the time-derivative of the vector state. Lastly, block *Integrator* generates the vector state, i.e., the vector

whose elements are x_{1m}, x_{2m}, x_{3m} along with its corresponding initial conditions.

- (ii) Sampling and scaling: With the aim of sending the vector state of the master system, a *Zero-Order Hold* is required for sampling the response of the system. Additionally, since the data are sent in 1 byte packages, a scaling factor is implemented through the *Scale* block so that the elements of the vector state are mapped into the interval $[0, 255]$.
- (iii) Data sending: All parameters for establishing the serial communication, such as velocity transmission, COM port, etc., are specified in the *Serial Configuration* block, whereas the *Conversion* block transforms double type data into uint8 type (equivalent to 1 byte). Lastly, data are sent through the COM port specified in the *Serial Send* block.

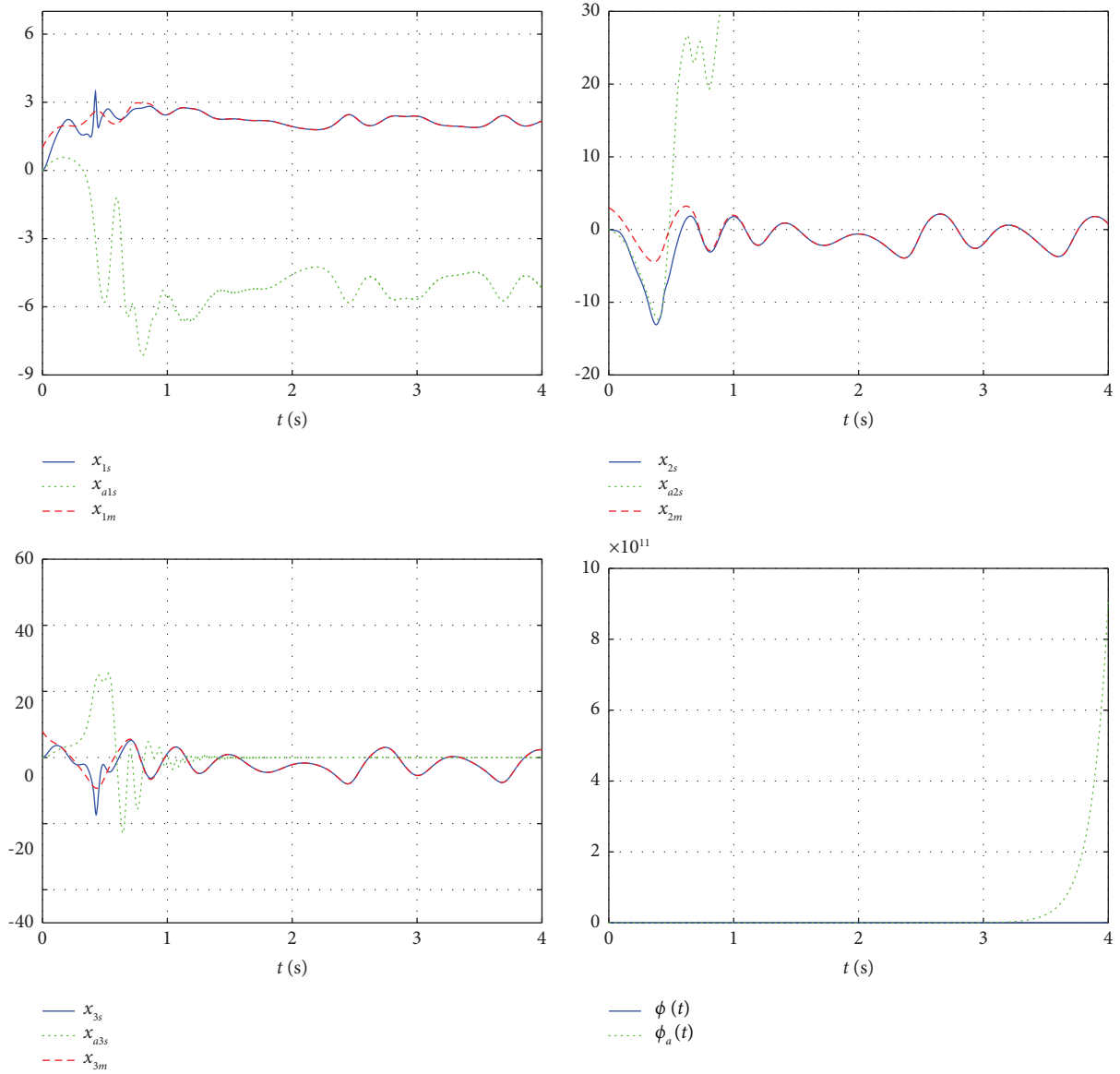


FIGURE 6: Numerical simulation 4. Results of the adaptive control and the active control in closed-loop with the Nwachioma chaotic system. The used parameters are in accordance with those specified on the fourth line in Table 1. The indexes obtained for this simulation are $\phi(10 \text{ s}) = 21.86$ and $\phi_a(10 \text{ s}) = 9.3 \times 10^{11}$.

TABLE 2: Performance indexes of the quadratic error integral for the numerical simulations.

	$\phi(t)$	$\phi_a(t)$	t (s)
Numerical simulation 1	11.11	97.48	10
Numerical simulation 2	14.76	899.70	10
Numerical simulation 3	18.57	4490	10
Numerical simulation 4	21.86	9.3×10^{11}	4

The index $\phi(t)$ represents the performance of the adaptive control, whereas the index $\phi_a(t)$ shows the performance of the active control.

On the other hand, the block diagram programmed in MATLAB-Simulink for implementing the slave system is presented in Figure 10 and is divided into the following parts:

- (i) Data receiving: In this block, the *Serial Configuration* is used again with the purpose of selecting the communication parameters. The *Serial Receive* acquires the uint8 data of the slave system, which are

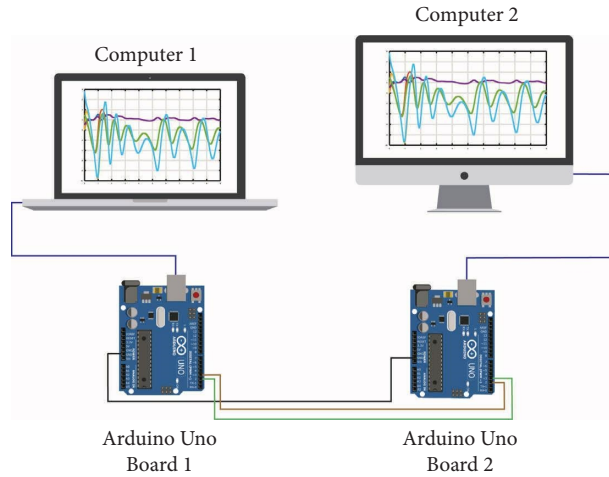


FIGURE 7: Experimental implementation of the Nwachioma chaotic system in the master-slave configuration. The master system and the slave system are implemented independently in two computers. The communication between both systems is realized through the protocol RS-232 via two Arduino UNO boards.

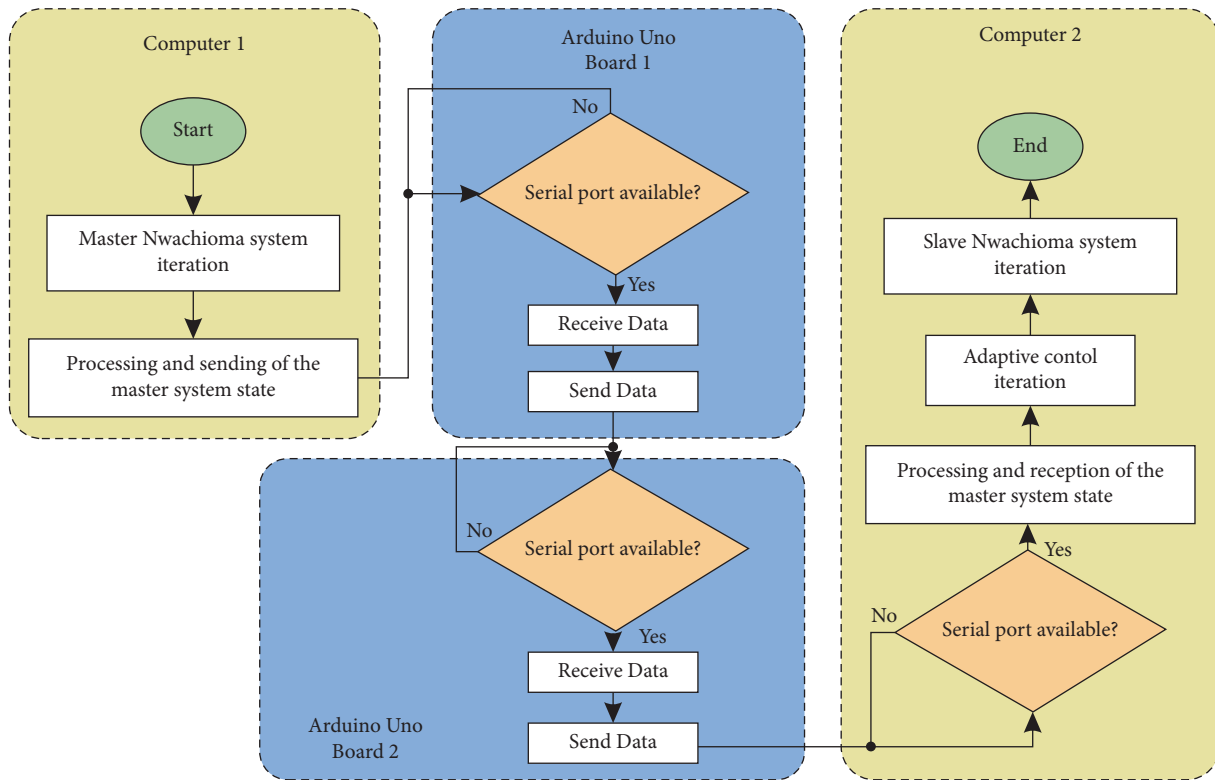


FIGURE 8: Flowchart for implementing the adaptive control on the Nwachioma chaotic system, in the master-slave configuration, through two computers and two Arduino UNO boards.

mapped in the scale $[0, 255]$, and by using the *Conversion* block the data are converted into type double. Later, the block *Scale* recovers the original scaling factor of the state vector.

(ii) Nwachioma slave system: It comprises the block of parameters a_i , where constants (2) are programmed again for implementation purposes. The block *Slave*

is where the equations (4) are programmed with the aim of obtaining the time-derivatives \dot{x}_{1s} , \dot{x}_{2s} , and \dot{x}_{3s} . The states x_{1s} , x_{2s} , and x_{3s} are obtained by considering the initial conditions of the slave system through the block *Integrator2*.

(iii) Learning law: Equations (13) are programmed into the block *Update law* with the intention of obtaining

```

#include <SoftwareSerial.h>
#define rxPin 2
#define txPin 3
SoftwareSerial VirtualSerial = SoftwareSerial(rxPin, txPin);
void setup()
{
  Serial.begin(9600);
  VirtualSerial.begin(9600);
}
void loop()
{
  byte InData;
  if (Serial.available())
  {
    InData = Serial.read();
    VirtualSerial.write(InData);
  }
  if(VirtualSerial.available())
  {
    InData = VirtualSerial.read();
    Serial.write(InData);
  }
}

```

LISTING 1: Arduino code programming language for implementing the RS-232 serial communication.

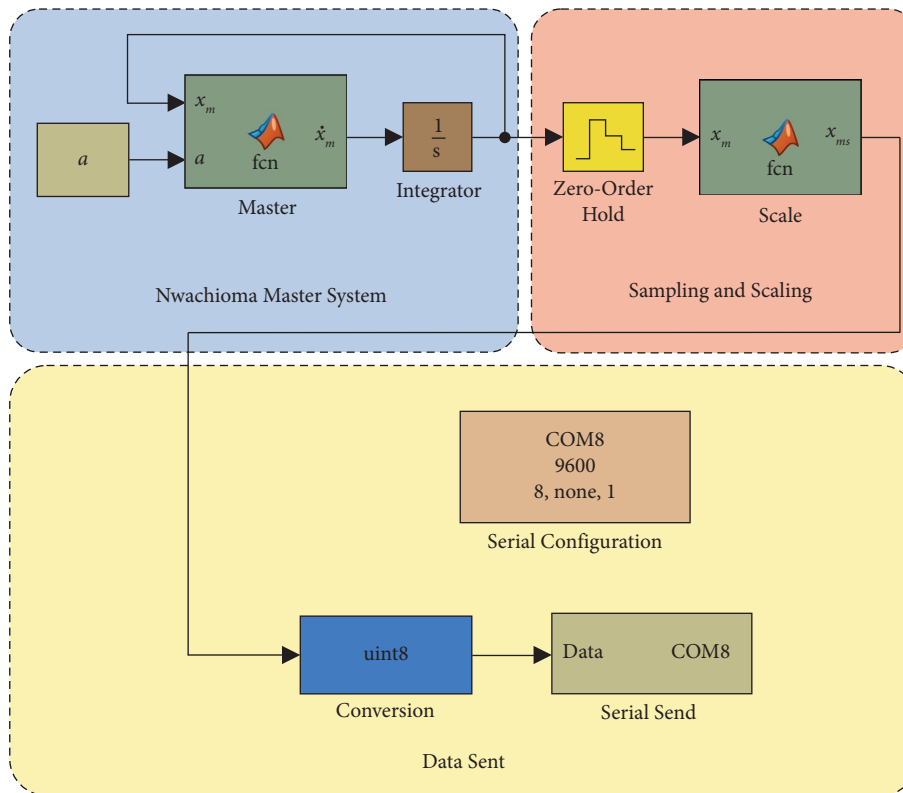


FIGURE 9: Block diagram programmed in MATLAB-Simulink for computer 1. With this program, the master system is implemented and the corresponding data associated with the states are sent via the communication protocol RS-232 to the slave system.

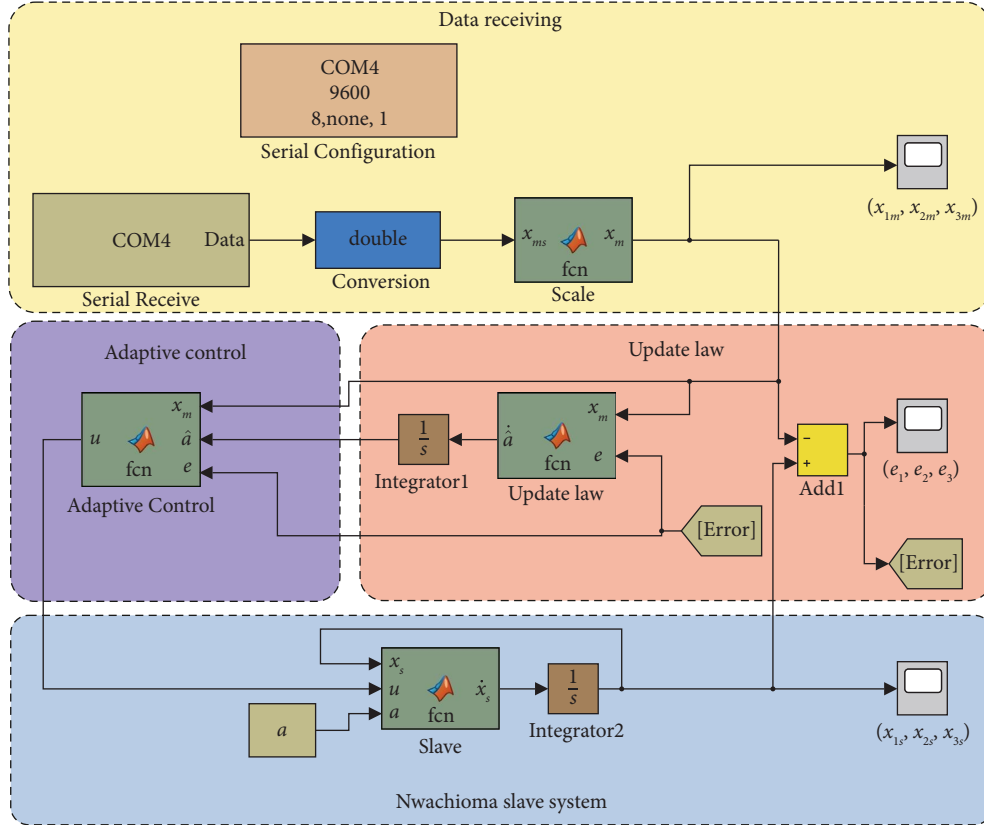


FIGURE 10: Block diagram programmed in MATLAB-Simulink for computer 2. With this program, the slave system is implemented, the data associated with the master system are acquired via the communication protocol RS-232, and the adaptive control is executed.

\hat{a}_i . It is easily observed that after using the block *Integrator1*, over the time-derivatives previously mentioned, the corresponding signals \hat{a}_i are obtained (after considering initial conditions equal to zero) and now can be used into the proposed adaptive control.

- (iv) Adaptive control: This block generates the corresponding inputs u_1 , u_2 , and u_3 through (9) and by taking into account, as parameters, the signals e_1 , e_2 , e_3 , the estimated ones \hat{a}_i , and the states x_{1m} , x_{2m} , and x_{3m} .

3.2.2. Experimental Results. The master system (3) is experimentally implemented in computer 1, where the parameters given in (2) and the initial conditions ($x_{1m}(0) = 1$, $x_{2m}(0) = 3$, and $x_{3m}(0) = 8$ retaken from [98]) for the Nwachiona system, are specified. On the other hand, the slave system (4) is implemented in computer 2 and the parameters given in (2) are used again. The initial conditions for the slave system are considered to be $x_{1s}(0) = 0$,

$x_{2s}(0) = 0$, and $x_{3s}(0) = 0$, whereas for the learning law, and the initial condition of the time-derivative of the estimated values, $\hat{a}_i = 0$. The gains of the proposed adaptive control are chosen to be $k_1 = 5$, $k_2 = 7$, and $k_3 = 5$. With all these values, the system in closed-loop achieves the synchronization objective, i.e., $(x_{1s}, x_{2s}, x_{3s}) \rightarrow (x_{1m}, x_{2m}, x_{3m})$, as can be observed in Figure 11.

Figure 12(a) shows that $(e_1, e_2, e_3) \rightarrow (0, 0, 0)$ even when the initial conditions of both systems are not equal, whereas Figure 12(b) depicts the control inputs of the slave system, whose behavior not only allows that $(e_1, e_2, e_3) \rightarrow (0, 0, 0)$ but also that $(u_1, u_2, u_3) \rightarrow (0, 0, 0)$.

3.2.3. Comments on the Experimental Results. As was previously mentioned, chaotic systems are very sensitive to initial conditions (this phenomenon can be observed in Figure 2). Notice that, in Figures 11 and 12, although such initial conditions are different in both, the master and the slave systems, the synchronization problem is solved. Also, despite the master-slave communication is low-cost and

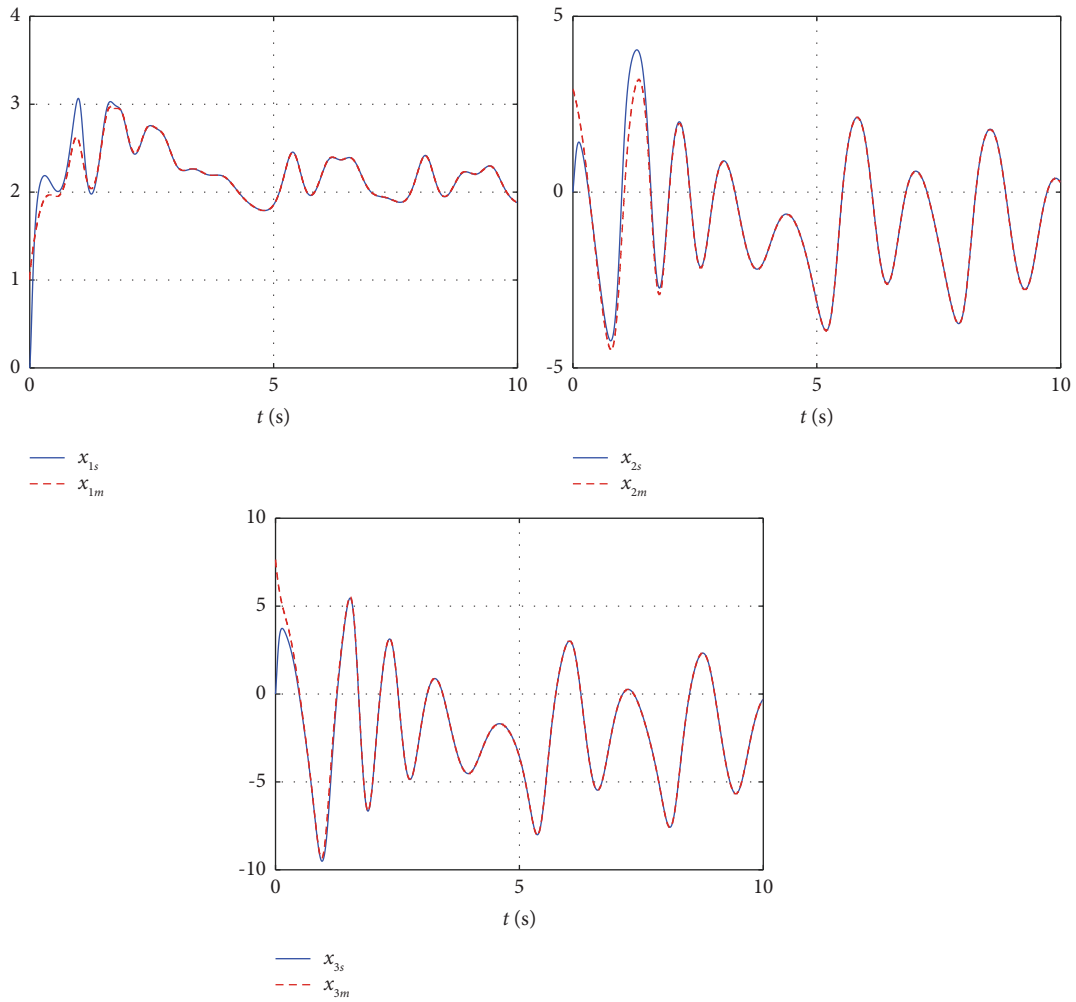


FIGURE 11: Experimental comparison between the states of the master system versus the corresponding states of the slave system. The initial conditions of the master system are $x_{1m}(0) = 1$, $x_{2m}(0) = 3$, and $x_{3m}(0) = 8$, whereas those of the slave system are $x_{1s}(0) = 0$, $x_{2s}(0) = 0$, and $x_{3s}(0) = 0$.

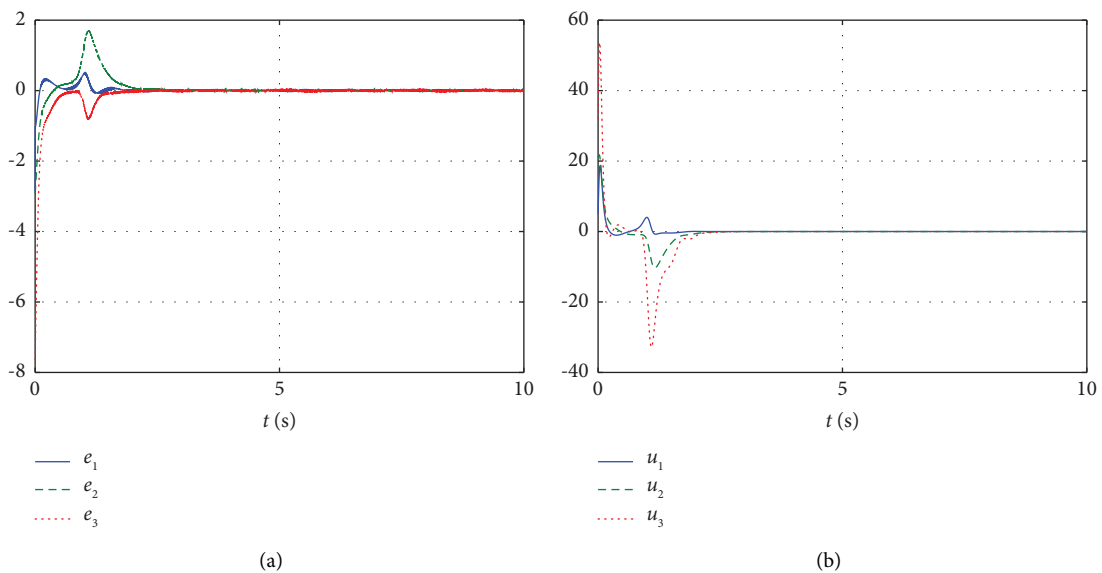


FIGURE 12: Experimental results indicators. (a) Synchronization errors of the Nwachioma master-slave system, described by (5). (b) Inputs of the slave system allowing that $(x_{1s}, x_{2s}, x_{3s}) \rightarrow (x_{1m}, x_{2m}, x_{3m})$ are achieved.

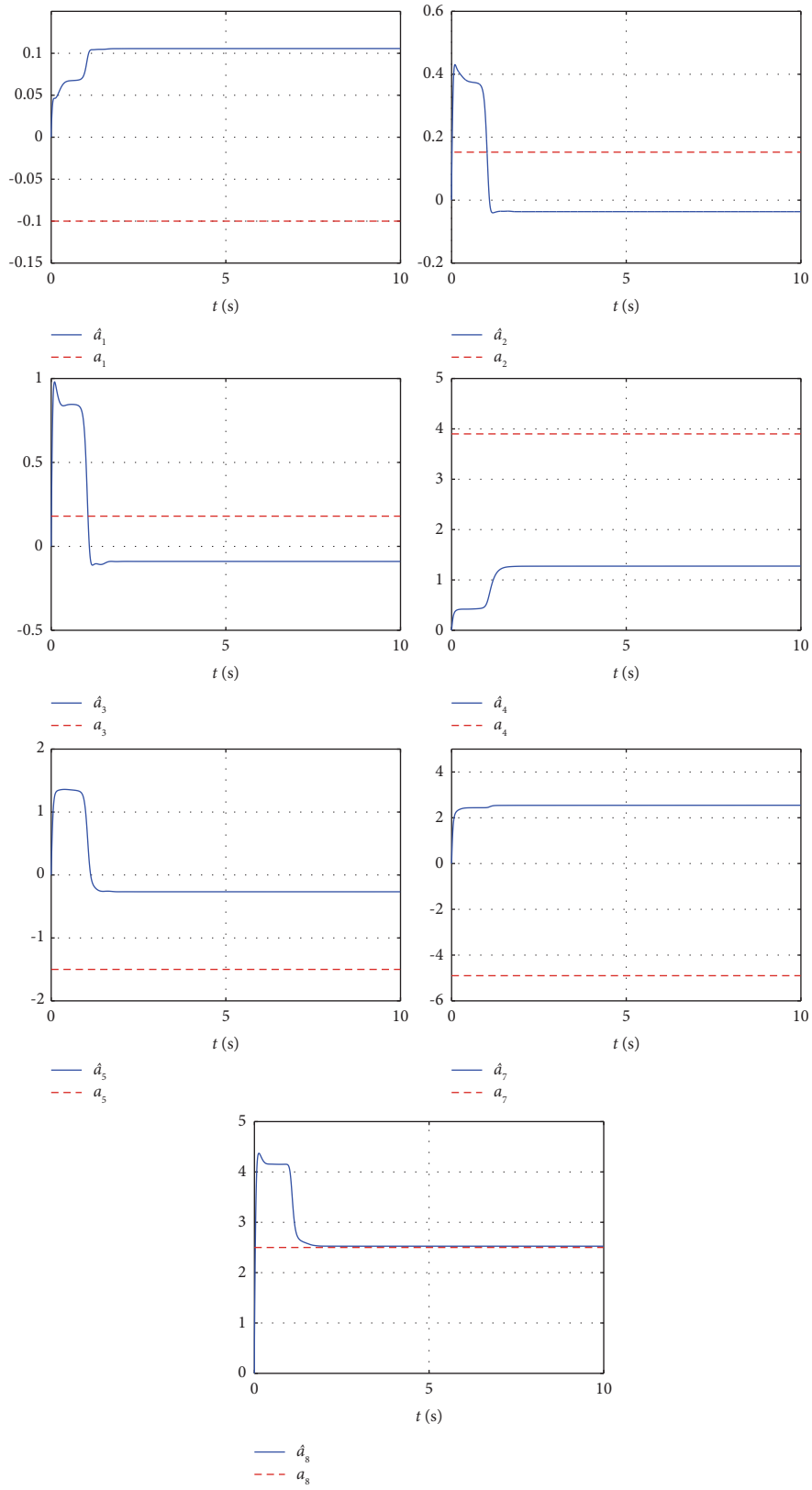


FIGURE 13: Comparison between the adaptive parameters \hat{a}_i of the proposed adaptive control and the constants a_i of the Nwachima system.

with communication delays, the synchronization is achieved in a short period of time. As depicted in Figure 13, although $\hat{a}_i \rightarrow a_i$ is not true, the errors $\tilde{a}_i = \hat{a}_i - a_i$ are bounded.

4. Conclusions and Future Work

For the first time in literature, an adaptive control algorithm for solving the synchronization task on the Nwachioma master-slave chaotic system was presented in this paper. The feasibility and performance of the closed-loop system were demonstrated in two senses. The first one was by comparing via numerical simulations the adaptive control with an active control by implementing them in closed-loop on the master-slave Nwachioma chaotic system via MATLAB-Simulink. The simulation results showed that the performance of the adaptive control is superior to the one obtained with the active control, i.e., $(x_{1s}, x_{2s}, x_{3s}) \rightarrow (x_{1m}, x_{2m}, x_{3m})$, and was verified through the performance indexes of the quadratic error integral associated with both controls in closed-loop. In all simulations, the parameters a_i of the master system and those of the slave system were different for both control algorithms. The second one was by executing the experimental implementation of the adaptive control on a testbed of the master-slave Nwachioma chaotic system. The experimental implementation of the master system was carried out on a computer via MATLAB-Simulink. This computer sent the states x_{1m} , x_{2m} , and x_{3m} through the Arduino UNO board and the RS-232 serial protocol. Then, the computer associated with the slave system received such states and executed the corresponding learning law and the adaptive control, also via MATLAB-Simulink, with the aim of solving the synchronization task. The experimental results showed that the proposed adaptive control achieves in finite time that $(x_{1s}, x_{2s}, x_{3s}) \rightarrow (x_{1m}, x_{2m}, x_{3m})$.

As a future work, the current results will be generalized to several slave systems synchronized only to one master system [107]. Also, a potential extension of the results presented in this paper could include external disturbances [108] on the Nwachioma chaotic system in the master-slave configuration.

Data Availability

The data used to support the findings of this study are available from the corresponding author upon request.

Conflicts of Interest

The authors declare that they have no conflicts of interest.

Acknowledgments

This work was supported by Secretaría de Investigación y Posgrado del Instituto Politécnico Nacional, Mexico, and SNI-CONACYT-Mexico.

References

[1] H. Tirandaz and S. Saeidaminabadi, "Identical and non-identical synchronization of three scroll unified chaotic system (TSUCS) with unknown parameter using a modified function projective control method," *Iranian Journal of*

Science and Technology - Transactions of Electrical Engineering, vol. 41, pp. 319–334, 2017.

[2] C. Nwachiona and J. H. Pérez-Cruz, "Realization and implementation of polynomial chaotic Sun system," *Physical Science International Journal*, vol. 16, pp. 1–7, 2018.

[3] G. Chen, "On some controllability conditions for chaotic dynamics control," *Chaos, Solitons & Fractals*, vol. 8, no. 9, pp. 1461–1470, 1997.

[4] L. M. Pecora and T. L. Carroll, "Synchronization of chaotic systems," *Chaos: An Interdisciplinary Journal of Nonlinear Science*, vol. 25, no. 9, pp. 097611–097612, 2015.

[5] E. N. Lorenz, "Deterministic nonperiodic flow," *Journal of the Atmospheric Sciences*, vol. 20, no. 2, pp. 130–141, 1963.

[6] A. A. Ewees, M. A. Elaziz, Z. Alameer, H. Ye, and Z. Jianhua, "Improving multilayer perceptron neural network using chaotic grasshopper optimization algorithm to forecast iron ore price volatility," *Resources Policy*, vol. 65, pp. 101555–101612, 2020.

[7] S. K. Palit and S. Mukherjee, "A study on dynamics and multiscale complexity of a neuro system," *Chaos, Solitons & Fractals*, vol. 145, pp. 110737–110810, 2021.

[8] J. Gao, C. Gu, and H. Yang, "Spiral waves with interfacial oscillatory chemical reactions emerge in a model of reaction-diffusion systems," *Chemical Physics*, vol. 528, pp. 110507–110516, 2020.

[9] K. M. Owolabi and B. Karaagac, "Chaotic and spatiotemporal oscillations in fractional reaction-diffusion system," *Chaos, Solitons & Fractals*, vol. 141, pp. 110302–110315, 2020.

[10] J. Luo, S. Qu, Z. Xiong, E. Appiagyei, and L. Zhao, "Observer-based finite-time modified projective synchronization of multiple uncertain chaotic systems and applications to secure communication using DNA encoding," *IEEE Access*, vol. 7, pp. 65527–65543, 2019.

[11] T. Karimov, D. Butusov, V. Andreev, A. Karimov, and A. Tutueva, "Accurate synchronization of digital and analog chaotic systems by parameters re-identification," *Electronics*, vol. 7, pp. 123–210, 2018.

[12] R. Babajans, D. Cirjulina, J. Grizans et al., "Impact of the chaotic synchronization's stability on the performance of QCPK communication system," *Electronics*, vol. 10, no. 6, pp. 640–714, 2021.

[13] L. Moysis, C. Volos, I. Stouboulos et al., "A novel chaotic system with a line equilibrium: analysis and its applications to secure communication and random bit generation," *Tele.com*, vol. 1, no. 3, pp. 283–296, 2020.

[14] A. S. Muhammad and F. S. I. E. A. Özkaynak, "SIEA: secure image encryption algorithm based on chaotic systems optimization algorithms and PUFs," *Symmetry*, vol. 13, no. 5, pp. 824–921, 2021.

[15] C. Wang, Y. Di, J. Tang, J. Shuai, Y. Zhang, and Q. Lu, "The dynamic analysis of a novel reconfigurable cubic chaotic map and its application in finite field," *Symmetry*, vol. 13, no. 8, pp. 1420–1424, 2021.

[16] O. Mofid, M. Momeni, S. Mobayen, and A. Fekih, "A disturbance-observer-based sliding mode control for the robust synchronization of uncertain delayed chaotic systems: application to data security," *IEEE Access*, vol. 9, pp. 16546–16555, 2021.

[17] B. Vaseghi, S. S. Hashemi, S. Mobayen, and A. Fekih, "Finite time chaos synchronization in time-delay channel and its application to satellite image encryption in OFDM communication systems," *IEEE Access*, vol. 9, pp. 21332–21344, 2021.

- [18] S. Hashemi, M. A. Pourmina, S. Mobayen, and M. R. Alagheband, "Multiuser wireless speech encryption using synchronized chaotic systems," *International Journal of Speech Technology*, vol. 24, no. 3, pp. 651–663, 2021.
- [19] K. Rajagopal, H. Jahanshahi, S. Jafari, R. Weldegiorgis, A. Karthikeyan, and P. Duraisamy, "Coexisting attractors in a fractional order hydro turbine governing system and fuzzy PID based chaos control," *Asian Journal of Control*, vol. 23, no. 2, pp. 894–907, 2020.
- [20] X. Xu and W. Guo, "Chaotic behavior of turbine regulating system for hydropower station under effect of nonlinear turbine characteristics," *Sustainable Energy Technologies and Assessments*, vol. 44, p. 101088, 2021.
- [21] L. Moysis, E. Petavratzis, M. Marwan, C. Volos, H. Nistazakis, and S. Ahmad, "Analysis, synchronization, and robotic application of a modified hyperjerk chaotic system," *Complexity*, vol. 2020, Article ID 2826850, pp. 1–15, 2020.
- [22] C. Nwachiona and J. H. Pérez Cruz, "Analysis of a new chaotic system, electronic realization and use in navigation of differential drive mobile robot," *Chaos, Solitons & Fractals*, vol. 144, pp. 1–12, 2021.
- [23] E. K. Petavratzis, C. K. Volos, L. Moysis et al., "An inverse pheromone approach in a chaotic mobile robot's path planning based on a modified logistic map," *Technologies*, vol. 7, no. 4, pp. 84–16, 2019.
- [24] E. Petavratzis, L. Moysis, C. Volos, I. Stouboulos, H. Nistazakis, and K. Valavanis, "A chaotic path planning generator enhanced by a memory technique," *Robotics and Autonomous Systems*, vol. 143, pp. 103826–1039, 2021.
- [25] S. Takougang Kingni, C. Alnamon, V. Kamdoum Tamba, and J. B. Chabi Orou, "Directly modulated semiconductor ring lasers: chaos synchronization and applications to cryptography communications," *Chaos Theory and Applications*, vol. 2, pp. 31–39, 2020.
- [26] R. Montero Canela, E. Zambrano Serrano, E. I. Tamariz Flores, J. M. Muñoz Pacheco, and R. Torrealba Meléndez, "Fractional chaos based-cryptosystem for generating encryption keys in Ad Hoc networks," *Ad Hoc Networks*, vol. 97, pp. 1–21, 2020.
- [27] J. Machicao, O. M. Bruno, and M. S. Baptista, "Zooming into chaos as a pathway for the creation of a fast, light and reliable cryptosystem," *Nonlinear Dynamics*, vol. 104, pp. 753–764, 2021.
- [28] S. Mobayen, C. Volos, and U. Cavusoglu, "A simple chaotic flow with hyperbolic sinusoidal function and its application to voice encryption," *Symmetry*, vol. 12, pp. 2047–2118, 2020.
- [29] B. Vaseghi, S. Mobayen, S. S. Hashemi, and A. Fekih, "Fast reaching finite time synchronization approach for chaotic systems with application in medical image encryption," *IEEE Access*, vol. 9, pp. 25911–25925, 2021.
- [30] J. Guo, Z. Zhao, F. Shi, R. Wang, and S. Li, "Observer-based synchronization control for coronary artery time-delay chaotic system," *IEEE Access*, vol. 7, pp. 51222–51235, 2019.
- [31] C. J. Ye, Z. Sharpe, and H. H. Heng, "Origins and consequences of chromosomal instability: from cellular adaptation to genome chaos-mediated system survival," *Genes*, vol. 11, no. 10, pp. 1162–1213, 2020.
- [32] J. M. Muñoz-Pacheco, C. Posadas-Castillo, and E. Zambrano-Serrano, "The effect of a non-local fractional operator in an asymmetrical glucose-insulin regulatory system: analysis, synchronization and electronic implementation," *Symmetry*, vol. 12, no. 9, pp. 1395–1422, 2020.
- [33] H. Jahanshahi, J. M. Muñoz-Pacheco, S. Bekiros, and N. D. Alotaibi, "A fractional-order SIRD model with time-dependent memory indexes for encompassing the multi-fractional characteristics of the COVID-19," *Chaos, Solitons & Fractals*, vol. 143, pp. 110632–110711, 2021.
- [34] S. Liu, N. Jiang, A. Zhao, Y. Zhang, and K. Qiu, "Secure optical communication based on cluster chaos synchronization in semiconductor lasers network," *IEEE Access*, vol. 8, pp. 11872–11879, 2020.
- [35] L. M. Pecora and T. L. Carroll, "Synchronization in chaotic systems," *Physical Review Letters*, vol. 64, no. 8, pp. 821–824, 1990.
- [36] E. W. Bai and K. E. Lonngren, "Synchronization of two Lorenz systems using active control," *Chaos, Solitons & Fractals*, vol. 8, no. 1, pp. 51–58, 1997.
- [37] E. W. Bai and K. E. Lonngren, "Sequential synchronization of two Lorenz systems using active control," *Chaos, Solitons & Fractals*, vol. 11, no. 7, pp. 1041–1044, 2000.
- [38] R. A. Tang, Y. L. Liu, and J. K. Xue, "An extended active control for chaos synchronization," *Physics Letters A*, vol. 373, no. 16, pp. 1449–1454, 2009.
- [39] M. T. Yassen, "Chaos synchronization between two different chaotic systems using active control," *Chaos, Solitons & Fractals*, vol. 23, no. 1, pp. 131–140, 2005.
- [40] J. H. Pérez-Cruz, E. A. Portilla-Flores, P. A. Niño-Suárez, and R. Rivera-Blas, "Design of a nonlinear controller and its intelligent optimization for exponential synchronization of a new chaotic system," *Optik*, vol. 130, pp. 201–212, 2017.
- [41] M. Varan and A. Akgul, "Control and synchronisation of a novel seven-dimensional hyperchaotic system with active control," *Pramana*, vol. 90, no. 4, pp. 54–58, 2018.
- [42] X. Zhu and W. S. Du, "New chaotic systems with two closed curve equilibrium passing the same point: chaotic behavior, bifurcations, and synchronization," *Symmetry*, vol. 11, no. 8, pp. 951–1010, 2019.
- [43] J. Sun, Y. Wang, Y. Wang, G. Cui, and Y. Shen, "Compound-combination synchronization of five chaotic systems via nonlinear control," *Optik*, vol. 127, no. 8, pp. 4136–4143, 2016.
- [44] S. Zheng, "Multi-switching combination synchronization of three different chaotic systems via nonlinear control," *Optik*, vol. 127, no. 21, pp. 10247–10258, 2016.
- [45] I. T. Hettiarachchi, S. Lakshmanan, A. Bhatti et al., "Chaotic synchronization of time-delay coupled Hindmarsh-Rose neurons via nonlinear control," *Nonlinear Dynamics*, vol. 86, no. 2, pp. 1249–1262, 2016.
- [46] V. K. Yadav, G. Prasad, M. Srivastava, and S. Das, "Combination-combination phase synchronization among non-identical fractional order complex chaotic systems via nonlinear control," *International Journal of Dynamics and Control*, vol. 7, no. 1, pp. 330–340, 2019.
- [47] V. K. Yadav, G. Prasad, M. Srivastava, and S. Das, "Triple compound synchronization among eight chaotic systems with external disturbances via nonlinear approach," *Differential Equations and Dynamical Systems*, vol. 30, no. 3, pp. 549–572, 2019.
- [48] A. Ouannas, S. Bendoukha, C. Volos, N. Boumaza, and A. Karouma, "Synchronization of fractional hyperchaotic Rabinovich systems via linear and nonlinear control with an application to secure communications," *International Journal of Control, Automation and Systems*, vol. 17, no. 9, pp. 2211–2219, 2019.
- [49] A. Abdurahman and H. Jiang, "Nonlinear control scheme for general decay projective synchronization of delayed

- memristor-based BAM neural networks,” *Neurocomputing*, vol. 357, pp. 282–291, 2019.
- [50] S. Y. Al-Hayali and S. F. Al-Azzawi, “An optimal control for complete synchronization of 4D Rabinovich hyperchaotic systems,” *Telkomnika*, vol. 18, no. 2, pp. 994–1000, 2020.
- [51] A. S. Al-Obeidi and S. F. Al-Azzawi, “Chaos synchronization in a 6-D hyperchaotic system with self-excited attractor,” *Telkomnika*, vol. 18, no. 3, pp. 1483–1490, 2020.
- [52] S. F. Al-Azzawi and A. S. Al-Obeidi, “Chaos synchronization in a new 6D hyperchaotic system with self-excited attractors and seventeen terms,” *Asian-European Journal of Mathematics*, vol. 14, no. 05, Article ID 2150085, 2021.
- [53] P. Trikha, L. S. Jahanzaib, Nasreen, and D. Baleanu, “Dynamical analysis and triple compound combination anti-synchronization of novel fractional chaotic system,” *Journal of Vibration and Control*, vol. 28, no. 9-10, pp. 1057–1073, 2021.
- [54] D. Lin, X. Chen, G. Yu, Z. Li, and Y. Xia, “Global exponential synchronization via nonlinear feedback control for delayed inertial memristor-based quaternion-valued neural networks with impulses,” *Applied Mathematics and Computation*, vol. 2021, Article ID 126093, 401 pages, 2021.
- [55] L. S. Jahanzaib, P. Trikha, and D. Baleanu, “Analysis and application using quad compound combination anti-synchronization on novel fractional-order chaotic system,” *Arabian Journal for Science and Engineering*, vol. 46, no. 2, pp. 1729–1742, 2021.
- [56] A. Ouannas, A. A. Khennaoui, Z. Odibat, V. T. Pham, and G. Grassi, “On the dynamics, control and synchronization of fractional-order Ikeda map,” *Chaos, Solitons & Fractals*, vol. 123, pp. 108–115, 2019.
- [57] F. Mesdoui, A. Ouannas, N. Shawagfeh, G. Grassi, and V. T. Pham, “Synchronization methods for the Degr-Harrison reaction-diffusion systems,” *IEEE Access*, vol. 8, pp. 91829–91836, 2020.
- [58] X. Wu, G. Chen, and J. Cai, “Chaos synchronization of the master-slave generalized Lorenz systems via linear state error feedback control,” *Physica D: Nonlinear Phenomena*, vol. 229, no. 1, pp. 52–80, 2007.
- [59] Z. Yan and P. Yu, “Linear feedback control, adaptive feedback control and their combination for chaos (lag) synchronization of LC chaotic systems,” *Chaos, Solitons & Fractals*, vol. 33, no. 2, pp. 419–435, 2007.
- [60] M. Rafikov and J. M. Balthazar, “On control and synchronization in chaotic and hyperchaotic systems via linear feedback control,” *Communications in Nonlinear Science and Numerical Simulation*, vol. 13, no. 7, pp. 1246–1255, 2008.
- [61] Y. Chen, X. Wu, and Z. Gui, “Global synchronization criteria for a class of third-order non-autonomous chaotic systems via linear state error feedback control,” *Applied Mathematical Modelling*, vol. 34, no. 12, pp. 4161–4170, 2010.
- [62] S. Mobayen and F. Tchier, “Synchronization of a class of uncertain chaotic systems with lipschitz nonlinearities using state-feedback control design: a matrix inequality approach,” *Asian Journal of Control*, vol. 20, no. 1, pp. 71–85, 2018.
- [63] Z. Zhao, F. Lv, J. Zhang, and Y. Du, “H ∞ Synchronization for Uncertain Time-Delay Chaotic Systems with One-Sided Lipschitz Nonlinearity,” *IEEE Access*, vol. 6, pp. 19798–19806, 2018.
- [64] E. E. Mahmoud, M. Higazy, and O. A. Althagafi, “A novel strategy for complete and phase robust synchronizations of chaotic nonlinear systems,” *Symmetry*, vol. 12, no. 11, pp. 1765–1818, 2020.
- [65] A. T. Azar, F. E. Serrano, Q. Zhu et al., “Robust stabilization and synchronization of a novel chaotic system with Input saturation constraints,” *Entropy*, vol. 23, no. 9, pp. 1110–1127, 2021.
- [66] N. Siddique and F.-U. Rehman, “Parameter identification and hybrid synchronization in an array of coupled chaotic systems with ring connection: an adaptive integral sliding mode approach,” *Mathematical Problems in Engineering*, vol. 2018, Article ID 6581493, 15 pages, 2018.
- [67] M. R. Mufti, H. Afzal, F. Ur-Rehman, W. Aslam, and M. I. Qureshi, “Transmission projective synchronization of multiple non-identical coupled chaotic systems using sliding mode control,” *IEEE Access*, vol. 7, pp. 17847–17861, 2019.
- [68] M. R. Mufti, H. Afzal, F.-U. Rehman, Q. R. Butt, and M. I. Qureshi, “Synchronization and antisynchronization between two non-identical chua oscillators via sliding mode control,” *IEEE Access*, vol. 6, pp. 45270–45280, 2018.
- [69] F. Nian, X. Liu, and Y. Zhang, “Sliding mode synchronization of fractional-order complex chaotic system with parametric and external disturbances,” *Chaos, Solitons & Fractals*, vol. 116, pp. 22–28, 2018.
- [70] C. Song, S. Fei, J. Cao, and C. Huang, “Robust synchronization of fractional-order uncertain chaotic systems based on output feedback sliding mode control,” *Mathematics*, vol. 7, pp. 599–610, 2019.
- [71] P. Y. Wan, T. L. Liao, J. J. Yan, and H. H. Tsai, “Discrete sliding mode control for chaos synchronization and its application to an improved El-Gamal cryptosystem,” *Symmetry*, vol. 11, no. 7, pp. 843–913, 2019.
- [72] K. A. Alattas, J. Mostafae, A. Sambah et al., “Nonsingular integral-type dynamic finite-time synchronization for hyper-chaotic systems,” *Mathematics*, vol. 10, pp. 115–122, 2021.
- [73] C. W. Wu, T. Yang, and L. O. Chua, “On adaptive synchronization and control of nonlinear dynamical systems,” *International Journal of Bifurcation and Chaos*, vol. 06, no. 03, pp. 455–471, 1996.
- [74] T. L. Liao, “Adaptive synchronization of two Lorenz Systems,” *Communicated by prof. Y. H. Ichikawa*, *Chaos, Solitons & Fractals*, vol. 9, pp. 1555–1561, 1998.
- [75] R. Behinfaraz, S. Ghaemi, and S. Khanmohammadi, “Adaptive synchronization of new fractional-order chaotic systems with fractional adaption laws based on risk analysis,” *Mathematical Methods in the Applied Sciences*, vol. 42, no. 6, pp. 1772–1785, 2019.
- [76] T. Wang, D. Wang, and K. Wu, “Chaotic adaptive synchronization control and application in chaotic secure communication for industrial internet of things,” *IEEE Access*, vol. 6, pp. 8584–8590, 2018.
- [77] J. H. Pérez-Cruz, “Stabilization and synchronization of uncertain zhang system by means of robust adaptive control,” *Complexity*, vol. 2018, Article ID 4989520, 19 pages, 2018.
- [78] A.-A. Khennaoui, A. Ouannas, S. Bendoukha, X. Wang, and V.-T. Pham, “On chaos in the fractional-order discrete-time unified system and its control synchronization,” *Entropy*, vol. 20, no. 7, pp. 530–615, 2018.
- [79] S. Luo, S. Li, F. Tajaddodianfar, and J. Hu, “Adaptive synchronization of the fractional-order chaotic arch micro-electro-mechanical system via Chebyshev neural network,” *IEEE Sensors Journal*, vol. 18, no. 9, pp. 3524–3532, 2018.
- [80] L. Xu, H. Ma, and S. Xiao, “Exponential synchronization of chaotic lur’e systems using an adaptive event-triggered mechanism,” *IEEE Access*, vol. 6, pp. 61295–61304, 2018.

- [81] R. Zhang, Y. Liu, and S. Yang, "Adaptive synchronization of fractional-order complex chaotic system with unknown complex parameters," *Entropy*, vol. 21, no. 2, pp. 207–212, 2019.
- [82] L. Liu, C. Du, X. Zhang, J. Li, and S. Shi, "Adaptive synchronization strategy between two autonomous dissipative chaotic systems using fractional-order mittag-leffler stability," *Entropy*, vol. 21, no. 4, pp. 383–419, 2019.
- [83] P. P. Singh and B. K. Roy, "Comparative performances of synchronisation between different classes of chaotic systems using three control techniques," *Annual Reviews in Control*, vol. 45, pp. 152–165, 2018.
- [84] Y. Gao, D. Ding, and Z. Tang, "Adaptive cluster synchronization of complex networks with identical and non-identical Lur'e systems," *Electronics*, vol. 9, no. 5, pp. 706–716, 2020.
- [85] A. T. Azar and F. E. Serrano, "Stabilization of port Hamiltonian chaotic systems with hidden attractors by adaptive terminal sliding mode control," *Entropy*, vol. 22, pp. 122–215, 2020.
- [86] A. A. K. Javan, A. Shoeibi, A. Zare et al., "Design of adaptive-robust controller for multi-state synchronization of chaotic systems with unknown and time-varying delays and its application in secure communication," *Electronics*, vol. 21, pp. 1–21, 2021.
- [87] A. A. K. Javan, M. Jafari, A. Shoeibi et al., "Medical images encryption based on adaptive-robust multi-mode synchronization of Chen hyper-chaotic systems," *Sensors*, vol. 21, no. 11, pp. 3925–3934, 2021.
- [88] Z. Wang and G. Rongwei, "Hybrid synchronization problem of a class of chaotic systems by an universal control method," *Symmetry*, vol. 10, pp. 1–18, 2018.
- [89] A. A. Khennaoui, A. Ouannas, S. Bendoukha et al., "Chaos, control, and synchronization in some fractional-order difference equations," *Advances in Difference Equations*, vol. 2019, p. 423, 2019.
- [90] Z.-A. S. A. Rahman, B. H. Jasim, Y. I. A. Al-Yasir, R. A. Abd-Alhameed, and B. N. Alhasnawi, "A new No equilibrium fractional order chaotic system, dynamical investigation, synchronization, and its digital implementation," *Inventions*, vol. 6, no. 3, p. 49, 2021.
- [91] Y.-M. Chu, S. Bekiros, E. Zambrano-Serrano et al., "Artificial macro-economics: a chaotic discrete-time fractional-order laboratory model," *Chaos, Solitons and Fractals*, vol. 145, Article ID 110776, 2021.
- [92] H. Takhi, K. Kemih, L. Moysis, and C. Volos, "Passivity based sliding mode control and synchronization of a perturbed uncertain unified chaotic system," *Mathematics and Computers in Simulation*, vol. 181, pp. 150–169, 2021.
- [93] A. Ouannas, A. A. Khennaoui, T. E. Oussaeif, V. T. Pham, G. Grassi, and Z. Dibi, "Hyperchaotic fractional Grassi-Miller map and its hardware implementation," *Integration*, vol. 80, pp. 13–19, 2021.
- [94] H. Hamiche, H. Takhi, M. Messadi, K. Kemih, O. Megherbi, and M. Bettayeb, "New synchronization results for a class of nonlinear discrete-time chaotic systems based on synergetic observer and their implementation," *Mathematics and Computers in Simulation*, vol. 185, pp. 194–217, 2021.
- [95] T. Bonny, "Chaotic or hyper-chaotic oscillator? Numerical solution, circuit design, MATLAB HDL-coder implementation, VHDL code, security analysis, and FPGA realization," *Circuits, Systems, and Signal Processing*, vol. 40, no. 3, pp. 1061–1088, 2021.
- [96] J. Wang, L. Xiao, K. Rajagopal, A. Akgul, S. Cicek, and B. Aricioglu, "Fractional-order analysis of modified Chua's circuit system with the smooth degree of 3 and its microcontroller-based implementation with analog circuit design," *Symmetry*, vol. 13, no. 2, pp. 340–413, 2021.
- [97] V. A. Adeyemi, J. C. Nuñez-Pérez, Y. Sandoval-Ibarra, F. J. Pérez-Pinal, and E. Tlelo-Cuautle, "FPGA realization of the parameter-switching method in the Chen oscillator and application in image transmission," *Symmetry*, vol. 13, no. 6, pp. 923–1021, 2021.
- [98] C. Nwachioma, J. Humberto Perez-Cruz, A. Jimenez, M. Ezuma, and R. Rivera-Blas, "A new chaotic oscillator—properties, analog implementation, and secure communication application," *IEEE Access*, vol. 7, pp. 7510–7521, 2019.
- [99] D. R. Merkin, *Introduction to the theory of stability*, Springer Science and Business Media, Berlin, Germany, 2012.
- [100] A. S. Pozniak, E. N. Sanchez, and W. Yu, *Differential Neural Networks for Robust Nonlinear Control: Identification, State Estimation and Trajectory Tracking*, World Scientific, Singapore, 2001.
- [101] A. S. Al-Obeidi, S. Fawzi Al-Azzawi, A. Abdullah Hamad et al., "A novel of new 7D hyperchaotic system with self-excited attractors and its hybrid synchronization," *Computational Intelligence and Neuroscience*, vol. 2021, Article ID 3081345, 11 pages, 2021.
- [102] A. S. Ishomrani, M. Z. Ullah, and D. Baleanu, "A new approach on the modelling, chaos control and synchronization of a fractional biological oscillator," *Advances in Difference Equations*, vol. 2021, pp. 1–20, 2021.
- [103] A. A. Velamore, A. Hegde, A. A. Khan, and S. Deb, "Dual cascaded fractional-order chaotic synchronization for secure communication with analog circuit realisation," in *Proceedings of the 2021 IEEE Second International Conference on Control, Measurement and Instrumentation (CMI)*, pp. 30–35, Kolkata, India, January 2021.
- [104] L. Yan, J. Liu, F. Xu, K. L. Teo, and M. Lai, "Control and synchronization of hyperchaos in digital manufacturing supply chain," *Applied Mathematics and Computation*, vol. 391, p. 391, Article ID 125646, 2021.
- [105] F. Aydogmus and E. Tosyali, "Master-slave synchronization in a 4D dissipative nonlinear fermionic system," *International Journal of Control*, vol. 95, no. 3, pp. 620–625, 2022.
- [106] C. Arduino, "Arduino reference," 2019, <https://www.arduino.cc/reference/en/language/functions/communication/serial/>.
- [107] S. Mobayen, A. Fekih, S. Vaidyanathan, and A. A. Sambas, "Chameleon chaotic systems with quadratic nonlinearities: an adaptive finite-time sliding mode control approach and circuit simulation," *IEEE Access*, vol. 9, pp. 64558–64573, 2021.
- [108] H. Karami, S. Mobayen, M. Lashkari, F. Bayat, and A. Chang, "LMI-observer-based stabilizer for chaotic systems in the existence of a nonlinear function and perturbation," *Mathematics*, vol. 9, no. 10, pp. 1128–1215, 2021.